Acknowledgments

Os meus agradecimentos:

Ao Doutor Nuno Empadinhas por me ter aceitado no seu grupo e orientado o meu trabalho, estando sempre disponível para partilhar conhecimentos relevantes e debater novas estratégias de abordagem ao trabalho.

À Professora Doutora Teresa Gonçalves pelo acesso incondicional ao seu laboratório.

À Doutora Susana Alarico pela constante disponibilidade em me ensinar e por todo o tempo dispensado com valiosas indicações e ajudas na elaboração de todo o trabalho.

À Ana, à Andreia, ao Diogo e à Daniela pelo companheirismo e espírito de entreajuda que criamos todos os dias no MM-7.

À Professora Doutora Paula Morais por assumir a responsabilidade interna pela Tese no Departamento de Ciências da Vida.

A todos os membros do MMYRG pelo companheirismo.

Ao Doutor Tiago Faria pela disponibilidade e apoio em algumas partes do trabalho.

À Mizutani Foundation for Glycoscience, Japão, é reconhecido o apoio financeiro através do Exploratory Glycoscience 19th Research Grant 120123.

À FCT-Fundação para a Ciência e a Tecnologia, Portugal, através de fundos nacionais FCT/MCTES (PIDDAC) e ao Fundo Europeu de Desenvolvimento Regional (FEDER) através do COMPETE–Programa Operacional Factores de Competitividade (POFC), projectos PTDC/BIA-PRO/110523/2009–FCOMP-01-0124-FEDER-014321 e PEst-C/SAU/LA0001/2013 por terem suportado financeiramente este trabalho.

Aos meus pais e ao meu irmão pelo apoio absoluto e incentivo constante todos os dias, principalmente quando às vezes cheguei a casa desanimada.

Aos meus amigos, nomeadamente à Teresa Lino e Margarida Coelho, pela verdadeira amizade, por todo o encorajamento e por me "desviarem" para cafés e jantares para poder aproveitar também este último ano de "boa vida".

Ao meu namorado, Filipe, pelo amor e carinho, mesmo longe esteve sempre presente, um suporte constante e incondicional no decorrer de todo o trabalho, sempre com uma palavra de força para não desistir.

A todos vós, o meu sincero obrigada!!

INDEX

Abstract

Mycobacterium tuberculosis is the most infamous member among mycobacteria, although this genus already contains over 160 species, many of which opportunistic pathogens. These nontuberculous mycobacteria (NTM) are ubiquitous inhabitants of soils and waters and the cause of atypical infections frequently acquired in natural and man-made environments namely water distribution systems and hospitals. The emergence of drug- and disinfectant-resistant strains claims for urgent measures to fight these pathogens.

The adaptive success and resilience of mycobacteria is intimately associated to a lipid-rich cell wall that includes a thick layer of mycolic acids, which is impermeable to many antimicrobial agents and an effective barrier to host defenses. Mycobacteria produce unique polymers namely the intracellular polysaccharides of methylglucose (MGLP) or methylmannose (MMP), which have indirect but crucial involvement in cell wall biogenesis as they modulate the synthesis of fatty-acids, the precursors of mycolic acids.

Although MGLPs and MMPs have been discovered decades ago, only recently have their biosynthetic pathways been investigated at the genetic detail. The primer for MGLP synthesis is glucosylglycerate (GG), which was shown to accumulate during growth in nitrogen-starved *M. smegmatis* but not in nitrogen-rich medium. The addition of a nitrogen source to nitrogen-restricted cultures led to depletion of GG, implying the existence of an enzyme for its hydrolysis.

We selected *M. hassiacum* to investigate the fate of GG during growth in nitrogen-depleted versus nitrogen-rich media. Since a hydrolase with GG-hydrolytic activity had recently been described in thermophilic bacteria, we probed this organism's genome and cloned the homologous gene. The purified recombinant GG hydrolase (GgH) specifically hydrolysed GG to glucose and glycerate at 42ºC and pH 5.7 (optimal conditions), with Mg^{2+} and KCl significantly enhancing activity and GgH stability. The enzyme exhibited Michaelis-Menten kinetics at 37, 42 and 50ºC with comparable catalytic efficiencies. The purified GgH showed a single 51.2 kDa band on denaturing electrophoresis, but behaved as a dimeric protein in solution with a molecular mass of about 108.9 ± 2.6 kDa in size-exclusion chromatography.

Since GgH activity likely depletes cellular GG and may represent a regulatory node in MGLP biosynthesis, the understanding of the regulation of its expression by nitrogen fluctuations is crucial. The unique biochemical features of a novel enzymatic function reported here, furthers our knowledge of mycobacterial metabolism, physiology and lifestyle, and may lead to new strategies to fight infections caused by these ominous bacteria.

Keywords: *Mycobacterium hassiacum*, glucosylglycerate, hydrolase, methylglucose lipopolysaccharide (MGLP)

Resumo

Mycobacterium tuberculosis é a espécie mais ameaçadora do género *Mycobacterium*, que à data inclui mais de 160 espécies, na sua maioria espécies ambientais designadas não-tuberculosas (MNT), que podem ser patogénios oportunistas. As MNT são habitantes ubíquos de solos e águas de ambientes naturais ou artificiais, incluindo sistemas de distribuição de águas e hospitais. O surgimento de estirpes resistentes a antibióticos e desinfectantes reforça a necessidade urgente de medidas para combater infecções provocadas por estes patógenios.

O sucesso adaptativo e resiliência das micobactérias está intimamente associado à sua parede celular rica em lípidos, que inclui uma espessa camada de ácidos micólicos, o que a torna uma estrutura impermeável a agentes antimicrobianos e uma importante barreira contra defesas dos hospedeiros. As micobactérias sintetizam polímeros únicos, incluindo os polissacáridos intracelulares de metilglucose (MGLP) e de metilmanose (MMP), que têm um papel crucial na biogénese da parede, uma vez que modulam a síntese de ácidos gordos, os precursores dos ácidos micólicos. Embora o MGLP e o MMP tenham sido descobertos há décadas, só recentemente as suas vias de biossíntese foram investigadas ao nível genético.

O precursor da síntese do MGLP é glucosilglicerato (GG), um metabolito acumulado por *M. smegmatis* em condições limitantes de azoto. A adição de uma fonte de azoto levou à diminuição dos níveis de GG, implicando a existência de uma enzima dedicada à hidrólise deste composto. Seleccionámos *M. hassiacum* para investigar a dinâmica de acumulação de GG durante o crescimento em meio com limitação de azoto *versus* meio rico em azoto. Uma vez que foi recentemente identificada uma enzima capaz de hidrolisar GG, o gene homólogo de *M. hassiacum* foi detectado no genoma e clonado. A GG hidrolase (GgH) recombinante hidrolisa GG em glucose e glicerato a 42ºC e pH 5.7 (condições óptimas). Os iões Mg^{2+} e KCl potenciam a actividade e a estabilidade da GgH. A enzima exibe cinética Michaelis-Menten a 37, 42 e 50ºC com eficiência catalítica comparável. A GgH apresenta-se com 51.2 kDa em gel desnaturante, mas comporta-se como um dímero de massa 108.9 ± 2.6 kDa em solução.

Sendo a GgH a possível responsável pelo consumo do GG intracelular e pela regulação da biossíntese do MGLP, estudos futuros para melhor compreender a regulação da expressão deste gene durante flutuações de azoto são essenciais. As características bioquímicas desta enzima descritas neste trabalho, contribuem para o conhecimento do metabolismo, da fisiologia e do modo de vida micobacteriano, podendo levar ao desenvolvimento de estratégias para combater as infecções provocadas por micobactérias.

Palavras-chave: *Mycobacterium hassiacum*, glucosilglicerato, hidrolase, lipopolissacárido de metilglucose (MGLP)

List of Abbreviations

AcTr - acyltransferase

AG - arabinogalactan

AMMPs - acetylated methylmanose polysaccharides

BCG - bacilleCalmette-Guérin

DGG - diglucosylglycerate

DggS - diglucosylglycerate synthase

FAS-I - fatty acid synthase I

FPLC - fast protein liquid chromatography

GG - glucosylglycerate

GGG - glucosylglucosylglycerate

GgH - glucosylglycerate hydrolase

Ggs - glucosylglycerate synthase

GH - glycoside hydrolase

GlgA - α-(1→4)-glycosyltransferase

GlgE - maltosyltransferase

GPG - glucosyl-3-phosphoglycerate

GpgS - glucosyl-3-phosphoglycerate synthase

GpgP - glucosyl-3-phosphoglycerate phosphatase

GT - glucosyltransferase

LAM - lipoarabinomannan

LM - lipomannan

M1P - maltose-1-phosphate

MAs - mycolic acids

Mak - maltokinase

MAPc - mycolic acids-arabinogalactan-peptidoglycan complex

MeTr - methyltransferase

MG - mannosylglycerate

MgHs - mannosylglycerate hydrolases

MGLPs - methylglucose lipopolysaccharides

mGpgP - mycobacterial glucosyl-3-phosphoglycerate phosphatase

MMPs - methylmanose polysaccharides

MpgP - mannosyl-3-phosphoglycerate phosphatase

NTM - nontuberculous mycobacteria

PG - peptidoglycan

PGM - phosphoglycerate mutase

PMPSs - polymethylated polysaccharides

RGM - rapidly-growing mycobacteria

SAM - S-adenosylmethionine

SGM - slowly-growing mycobacteria

TB - tuberculosis

TLC - thin-layer chromatography

TreS - trehalose synthase

CHAPTER 1 - INTRODUCTION

1.1 Tuberculosis

Tuberculosis (TB) infects about one-third of world's population and is responsible for over two million deaths every year (Takayama et al., 2005; Mendes et al., 2012). This disease is difficult to control because its etiological agent, *Mycobacterium tuberculosis*, is easily disseminated when infected people cough and release droplets carrying the bacilli that are inhaled by uninfected persons (Glickman et al., 2001). Another obstacle against TB control is the difficulty in treating patients in developing countries. The recent escalation of multi- and extensively drug-resistant forms of TB and the emergence of new strains resistant to everything we have in our antibiotic arsenal, also poses a major threat to global health, especially due to the absence of new and effective chemotherapeutic options in the short-term (Dye, 2009).

The human immune system is highly efficient in responding and controlling the primary TB infection. However, *M. tuberculosis* has a remarkable capacity to remain latent within a seemingly healthy individual for decades without expression of symptoms before reactivating into active TB (Glickman et al., 2001; Fortune & Rubin, 2007). This microorganism has the ability to manipulate macrophage biology, since it inhibits vacuolar acidification and blocks phagolysosomal fusion, creating a protected niche where it can persist and replicate, contributing to the pathogenic persistence of the bacterium (Fortune & Rubin, 2007). Virulent strains are capable to evade the necrotic macrophage and spread to uninfected macrophages or to persist extracellularly, a hallmark of advanced pulmonary TB (Lee et al., 2011).

There is only one 80-year old vaccine available against TB, developed from an attenuated strain of *Mycobacterium bovis*, the bacilli Calmette-Guérin (BCG). It is urgent to discover new vaccines and antibiotics with faster, safer and wider therapeutic action (Russell et al., 2010).

1.2 The genus *Mycobacterium*

Over one hundred and sixty different species of *Mycobacterium* have been described so far and classified (http://www.bacterio.cict.fr/m/mycobacterium.html). This genus is included in the *Mycobacteriaceae* family, order *Actinomycetales* and class *Actinobacteria* (Shinnick & Good,

1994). Mycobacteria are rod-shaped, aerobic, non-motile and non-sporulating organisms and they have a hydrophobic cell wall rich in lipids (Rastogi et al., 2001). This genus includes obligate intracellular pathogens and environmental saprophytic species that may be opportunistic pathogens, which are commonly designated nontuberculous mycobacteria (NTM) to distinguish them from those species capable to cause tuberculosis (Rastogi et al., 2001).

Many mycobacteria infect humans and animals: *Mycobacterium leprae* causes leprosy and the species within the *M. tuberculosis* complex (*M. tuberculosis, M. bovis, M. africanum, M. microti, M. caprae*, *M. pinnipedii* and the two most recent members *M. mungi* and *M. orygis*) can cause tuberculosis in humans (Cousins et al., 2003; van Ingen et al., 2012). Recent studies confirmed that NTM can be pathogenic in particular conditions when immune system surveillance is impaired with immune deficiencies such as HIV-AIDS, cancer and chemotherapy, or immune depression during pregnancy, in toddlers and in the elderly, or due to transplants, chronic lung disease or even in cases of alcoholism and smoking (Falkinham, 2009; Weiss & Glassroth, 2012). Human to human NTM transmission has never been reported (McGrath et al., 2010). The high number of infections with NTM stems from the interference of humans with the environment, contributing to the proliferation and selection of NTM species (Falkinham, 2009).

Mycobacteria are traditionally divided in two groups: the slowly-growing mycobacteria (SGM) and the rapidly-growing mycobacteria (RGM) (Fig. 1). This classification is based on the time required by each species to form visible colonies on solid medium. RGM species need less than 7 days, while SGM species need more than 7 days and sometimes several weeks to form visible colonies on agar plates (Primm et al., 2004). Most pathogenic mycobacteria belong to the SGM group, while environmental saprophytic mycobacteria are more frequently RGM species (Shinnick & Good, 1994). The phylogenetic grouping based on 16S rRNA gene sequences also corroborates the RGM/SGM separation, with only a few exceptions (Fig. 1).

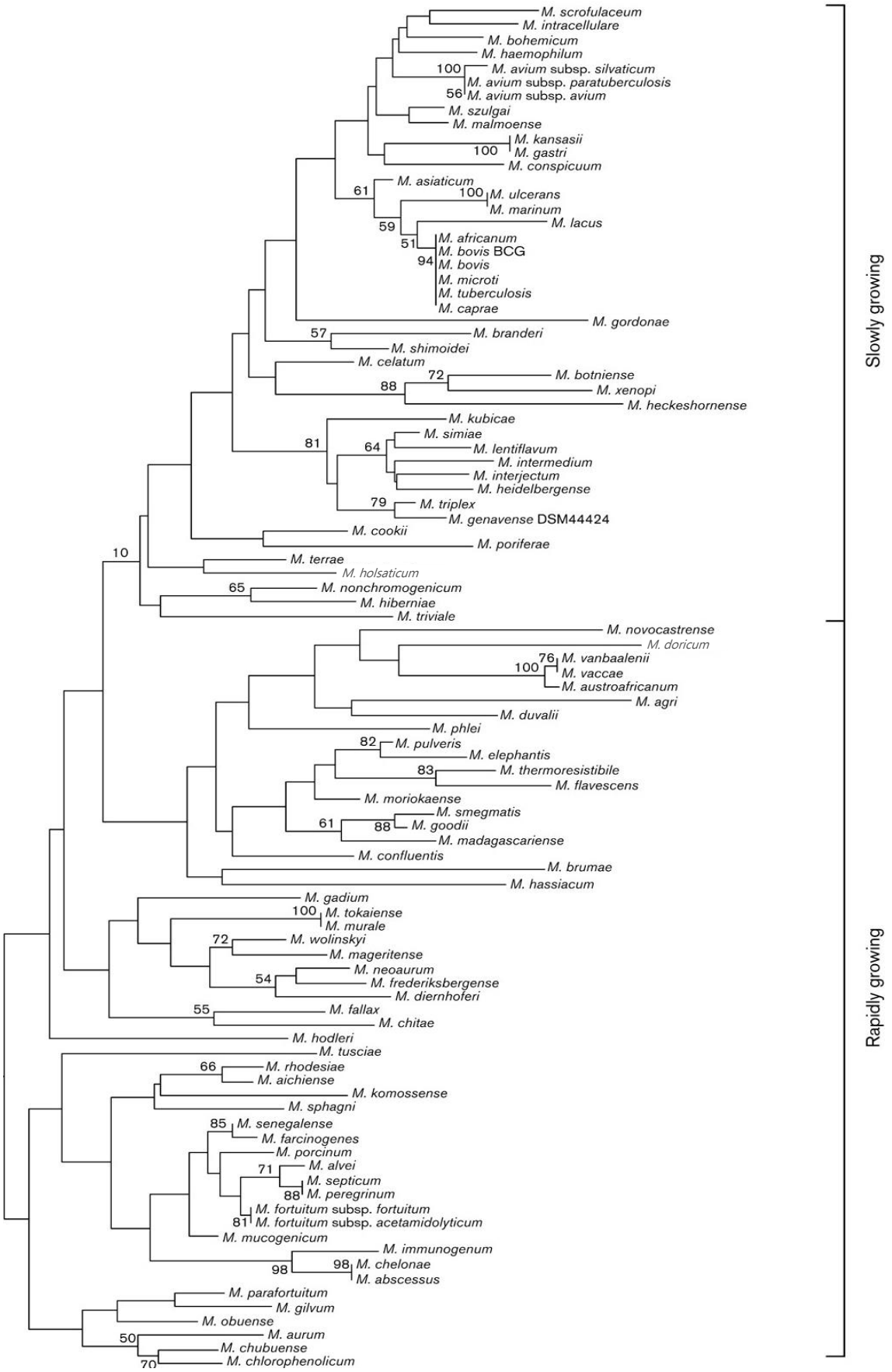

Figure 1 - Phylogenetic tree of the genus *Mycobacterium* constructed from 16S rRNA gene sequences. (adapted from Devulder et al., 2005).

1.2.1 Nontuberculous mycobacteria (NTM)

NTM are environmental species that are frequently isolated from habitats in contact with humans and animals such as soil, water, plants and dust (Tortoli, 2009). These environmental mycobacteria have different colony morphologies, growth rates, antibiotic and biocide sensitivities, plasmid carriage and virulence, but all of them have a high hydrophobic capacity conferred by compounds in their unique cell wall (Primm et al., 2004). Moreover, these mycobacteria are oligotrophs (able to grow in locals with low concentration of nutrients), have a high tolerance to extreme temperatures and pH, are capable to form biofilms and have a fast metabolism that allows rapid adaptation to adverse conditions (Primm et al., 2004; Falkinham, 2009; El Helou et al., 2013). These characteristics of NTM support a ubiquitous distribution in the environment and a high spectrum of adaptation also to different hosts, humans included, where they are an increasingly important cause of disease as opportunistic pathogens.

Water is considered the main source of NTM infection in humans because both RGM and SGM can colonize natural waters and artificial water distribution systems (Falkinham, 2009). Some NTM are thermotolerant (they can survive and disseminate in hot waters), namely members of the *Mycobacterium avium* complex (composed by *M. avium* and *M. intracellulare*), *M. xenopi, M. phlei* and *M. chelonae,* whereas others like *M. kansasii*, *M. abcessus* and *M. fortuitum* prefer cold waters (Phillips & Reyn, 2001; Primm et al., 2004; El Helou et al., 2013). Human activity and reckless discharge of chlorine, biocides, disinfectants and antibiotics in water also influence the growth and resilience of NTM, because selection of naturally resistant bacteria prevails with only a few sensitive bacteria being eliminated. Thus, NTM survive and persist in waters after disinfection and can further evolve adaptive resistance through the formation of biofilms (Falkinham, 2009). For example, the contamination of water allows NTM to form enriched biofilms in showerheads and be the source of infections (Feazel et al., 2009).

The members of the *M. avium* complex are the dominant cause of NTM pulmonary infections, followed by *M. kansasii* and *M. abcessus* (McGrath et al., 2010). Moreover, patients admitted to hospitals are frequent targets for infection (nosocomial) including those undergoing

dialysis treatments, due to contaminated solutions or reusable haemodialysis filters, or even after surgical procedures due to inadequate sterilization and disinfection of equipment. Infections can also take place through the use of reusable injection devices and contaminated syringes (Phillips & Reyn, 2001). Moreover, NTM can cause skin and lung infections, lymphadenitis and gastrointestinal disease (McGrath et al., 2010). The third most common mycobacterial disease worldwide is Buruli ulcer, which is caused by *M. ulcerans*. This is an endemic disease to many developing countries and rare in the western societies that results from contact with contaminated water or infected fish. It manifests itself as a cutis infection with destruction of skin and muscle and bone corrosion through the action of a necrotizing toxin. This species can actively grow in rivers and lakes at temperatures below 32ºC (Tortoli, 2009).

Many species of NTM remain to be described as their numbers in the environment may be too low to be detected accidentally. However, the constant pressure exerted by humans on ecosystems and the discharge of antibiotics, disinfectants and biocides in water streams will inevitably lead to an enrichment of potential mycobacterial pathogens in human environments.

1.2.1.1 *Mycobacterium hassiacum*

Mycobacterium hassiacum is a RGM of the NTM group that was isolated from the human urine of two asymptomatic patients (Schröder et al., 1997). Only recently *M. hassiacum* has been confirmed as an opportunistic cause of severe peritonitis in a patient undergoing peritoneal dialysis (Jiang et al., 2012). Its optimal growth temperature is 50ºC, but it can grow between 30ºC and 65ºC, reason why it was considered the most thermophilic species within the genus *Mycobacterium* (Schröder et al., 1997; Tiago et al., 2012).

A major obstacle to further understand mycobacterial biology is the characterization of their genetic and enzymatic resources as well as their biochemical pathways, mainly because proteins are difficult to purify from native hosts and their recovery from recombinant sources in stable and soluble bioactive form is also challenging (Mendes et al., 2011). Consequently, more than half of the predicted genes in *M. tuberculosis* genome remain to be associated to genuine

functions (TubercuList [http://tuberculist.epfl.ch/]) (Lew et al., 2011). The genome of the thermophilic species *M. hassiacum* was sequenced mainly because its inherently thermostable proteins are appealing for functional studies (Tiago et al., 2012). *Mycobacterium hassiacum* is also a suitable surrogate model to study *M. tuberculosis* enzymology because it is easy to grow *in vitro* and lacks the limitations imposed by the biosafety level 3 pathogen (*M. hassiacum* is a biosafely level 2 organism). Since sample stability is a major determinant in the success of crystallization trials and X-ray crystallography-based structure determination, *M. hassiacum* proteins also offer important tools in protein crystallization trials toward structure-guided drug discovery (Jenney Jr & Adams, 2008; Tiago et al., 2012).

1.3 The mycobacterial cell wall

The lipid-rich mycobacterial cell wall is an exclusive feature of the *Mycobacteriaceae* family. It confers these microorganisms a high hydrophobicity and resistance to antibiotics and disinfectants, which contributes to their pathogenicity and survival in inhospitable environments (Takayama et al., 2005; Hett & Rubin, 2008; Lopez-Marin, 2012). The cell wall surrounds the cytoplasmic membrane and is divided in an outer and an inner layer (Fig. 2). The outer layer, also called capsule, consists of carbohydrates, proteins, lipids and lipoglycans, namely lipoarabinomannan (LAM), lipomannan (LM), phthioceroldimycocerosate, dimycolyl trehalose, and phosphatidylinositol mannosides (Kaur et al., 2009). This layer plays an important role in the interaction with the host immune system (Hett & Rubin, 2008; Lopez-Marin, 2012). The inner layer extends outwards from the plasma membrane and is composed of covalently linked peptidoglycan (PG), arabinogalactan (AG) and mycolic acids (MAs), forming the MAP complex (MAPc), which forms an insoluble structure that is associated with the low-permeability of these organism's cell wall and their virulence (Fig. 2) (Hett & Rubin, 2008).

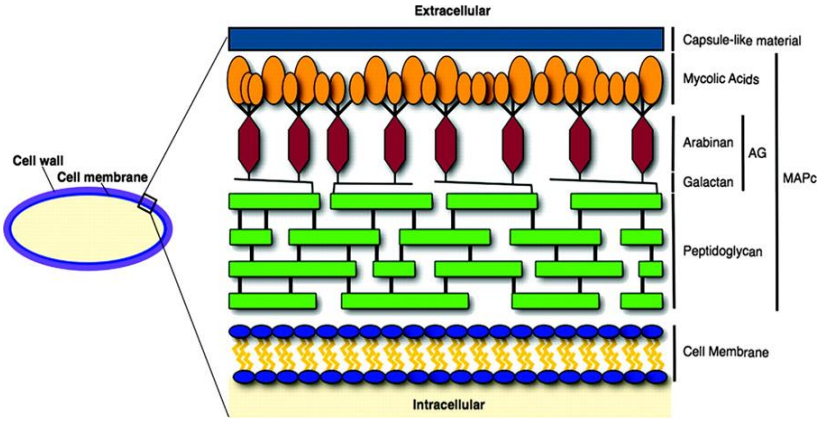

Figure 2 - Schematic representation of mycobacterial cell wall's structure (Hett& Rubin, 2008).

Peptidoglycan is a robust and elastic polysaccharide common to the majority of bacteria, which allows maintenance of cell shape and resistance to osmotic challenges. In mycobacteria, PG is linked through phosphodiester bonds to AG, the central constituent linking PG and MAs. Arabinogalactan is the main polysaccharide of the mycobacterial cell wall (Hett & Rubin, 2008). Mycolic acids are very long branched fatty acids, ranging between 60 and 90 carbons per chain, which can be organized in three structural classes: the α-mycolic, methoxy-mycolic acids and keto-mycolic acids (Takayama et al., 2005; Hett & Rubin, 2008). A study with *M. smegmatis* mutant strains unable to fully elongate MAs revealed that it is less resistant to drugs and temperature (Lopez-Marin, 2012). Moreover, a *M. tuberculosis* mutant deleted in cyclopropane ring of keto-mycolic acids showed a reduction of growth within macrophages (Takayama et al., 2005). In essence, MAs are essential for *Mycobacterium* biology (Takayama et al., 2005; Hett & Rubin, 2008; Lopez-Marin, 2012).

1.4 Polymethylated Polysaccharides

Mycobacteria synthesize unique and rare carbohydrates, including intracellular polymethylated polysaccharides (PMPSs) of 10 to 20 hexose units, most of them *O*-methylated, which confers them a slight hydrophobicity (Jackson & Brennan, 2009).

There are two types of PMPSs: the acylated methylglucose lipopolysaccharides (MGLPs) and the methylmannose polysaccharides (MMPs). Both types assume an helical conformation

in solution typical of amylose (Jackson & Brennan, 2009). The slightly hydrophobic "tunel" formed by the inward facing methyl groups allows PMPSs to establish stable 1:1 complexes with fatty acids and acyl-CoAs that protect them from degradation by cytoplasmic esterases (Fig. 3) (Jackson & Brennan, 2009). The sequestration of nascent acyl chains also stimulates the activity of fatty acid synthase I (FAS-I) making PMPSs crucial regulators of fatty acid synthesis, the essential building blocks of cell wall MAs (Ilton et al., 1971; Banis et al., 1977).

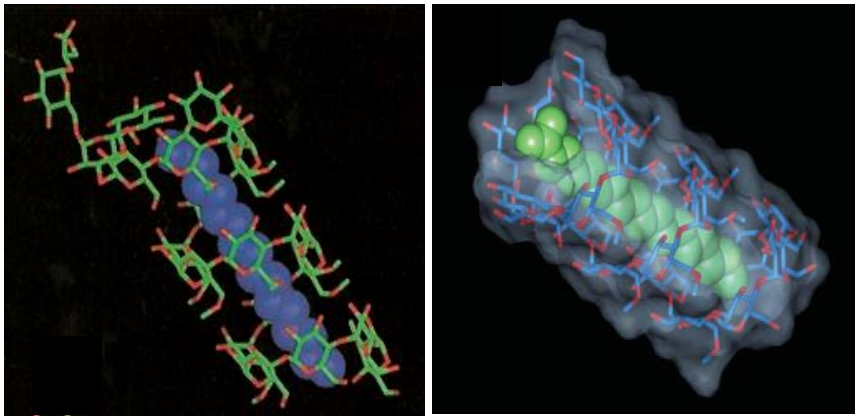

Figure 3 - Schematic representations of MGLP with a "docked" C16 fatty acid (adapted from Tuffal et al., 1995 and from Jackson & Brennan, 2009).

MGLPs are composed of 15 to 20 α-(1→4)-linked glucoses and 6-*O*-methylglucose units, some of which are acylated with acetate, propionate, isobutyrate, succinate and octanoate. MGLPs reducing end is composed of glyceric acid linked through an α-(1→2) linkage to the 1st glucose unit in the polysaccharide to form glucosylglycerate (GG). This GG unit is linked to the glucose that initiates the α-(1→4) main chain of MGLP by a α-(1→6) linkage. The 1st and 3rd glucoses of the main chain have branched β-(1→3)-linked glucoses and the non-reducing terminus of MGLP is a 3-*O*-methylglucose (Fig. 4) (Tuffal et al., 1998; Mendes et al., 2012).

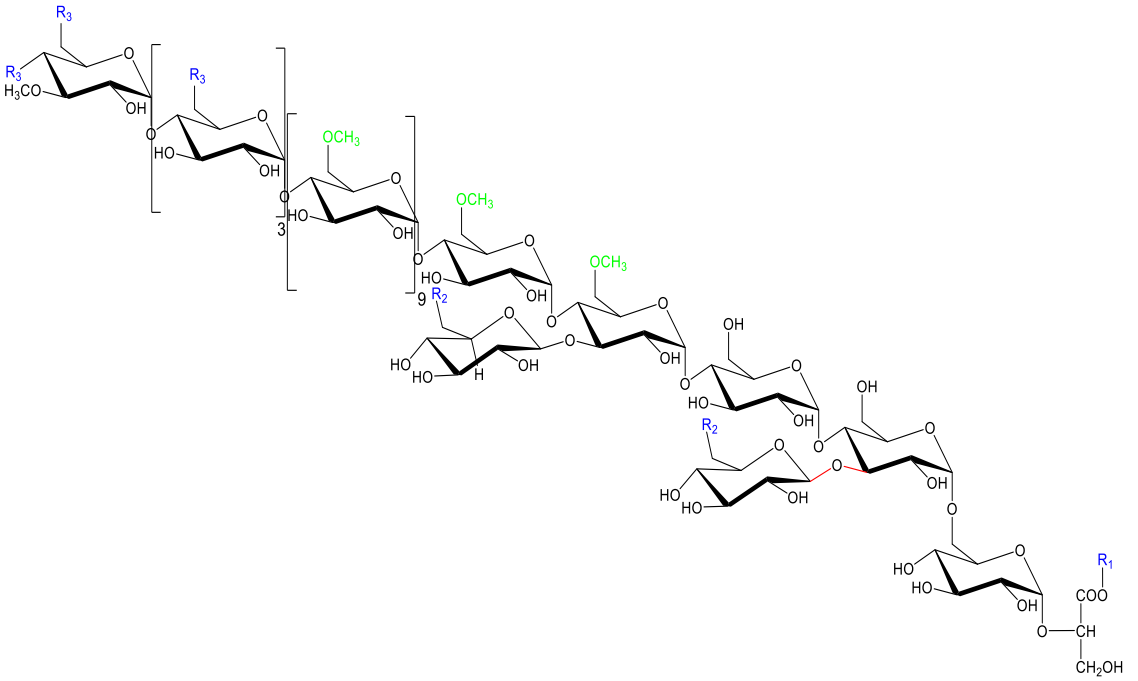

Figure 4 - Structure of a “linearized” MGLP (adapted from Mendes et al., 2012).
R_1, R_2 and R_3 are short-chain fatty acids.

MMPs are made of 10-13 non-acylated 3-*O*-methylmannoses, forming a linear chain linked by α-(1→4) linkages. The reducing end is blocked by a methyl aglycon, whereas the non-reducing end has an unmethylated mannose (Fig. 5) (Maitra & Ballou, 1977; Weisman & Ballou, 1984).

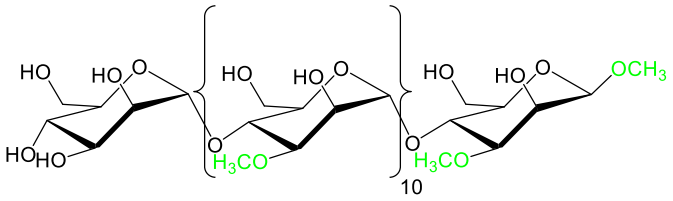

Figure 5 - Structure of a “linearized” MMP (adapted from Mendes et al., 2012).

MGLPs have been detected both in SGM and RGM and in several related *Nocardia* species (Table 1) (Pommier & Michel, 1986) whereas MMPs have only been isolated from RGM (Table 1) and from the related *Streptomyces griseus* (Harris & Gray, 1977). A striking difference between the mycobacterial and the *Streptomyces* MMPs is that the former are non-acylated molecules while the latter have esterified acetyl moieties, hence designated acetylated MMPs

(AMMPs) (Harris & Gray, 1977). Since PMPSs seem to be almost exclusively restricted to mycobacteria, they are attractive targets for new drugs against mycobacterioses. Since MGLPs seem to be the only type of PMPSs present in pathogenic SGM such as *M. tuberculosis* (Table 1) and due to their likely essential role, their biosynthetic machinery represent attractive targets for development of new drugs against tuberculosis (Mendes et al., 2012).

Table 1: MGLPs and MMPs isolated from *Mycobacterium* species

Mycobacterium SPECIES	GROWTH	MGLPS	MMPS	REFERENCES
M. tuberculosis	SGM	x		(Lee, 1966)
M. leprae	SGM	x		(Hunter et al., 1986)
***M. bovis* BCG**	SGM	x		(Tuffal et al., 1998)
M. xenopi	SGM	x		(Tuffal et al., 1995)
M. smegmatis	RGM	x	x	(Kamisango et al, 1987; Bergeron et al., 1975; Weisman & Ballou, 1984)
M. phlei	RGM	x	x	(Lee, 1966; Gray & Ballou, 1971)(Weisman & Ballou, 1984)
M. chitae	RGM	x	x	(Weisman & Ballou, 1984)
M. petrophilum	RGM	x	x	(Weisman & Ballou, 1984)
M. cuneatum	RGM	x	x	(Weisman & Ballou, 1984)
M. parafortuitum	RGM	x	x	(Weisman & Ballou, 1984)

1.5 Biosynthesis of MGLPs

The initial model proposed for MGLPs biosynthesis operates from the reducing end towards the non-reducing terminus of the polysaccharide with sequential glucosylation-methylation reactions for elongation of the main chain (Kamisango et al., 1987). The acylation of glucoses and branching events are unknown (Mendes et al., 2012). Glucosylglycerate (GG) was detected in *M. smegmatis* extracts and proposed to be the initial precursor for MGLP synthesis (Kamisango et al., 1987) (see section 1.5.1). The 2nd step was suggested to be the formation of diglucosylglycerate (DGG), as it was also detected in the extracts (Kamisango et al., 1987). The putative di-glucosylglycerate synthase (DggS) was proposed to be a glycoside

hydrolase of the GH57 family (www.cazy.org), encoded by gene *Rv3031* in *M. tuberculosis* H37Rv (Fig. 6), although this possibility lacks experimental confirmation (Stadthagen et al., 2007; Jackson & Brennan, 2009). The elongation of MGLP was considered to be catalyzed by an α-(1→4)-glycosyltransferase encoded by *Rv3032* (Stadthagen et al., 2007) found in the same operon (Fig. 6). This gene was considered essential for *M. tuberculosis* growth (Sassetti et al., 2003), but a *Rv3032* mutant synthesized trace levels of MGLP, which revealed the existence of an alternative enzyme with compensatory activity (Stadthagen et al., 2007). One such possible enzyme is the α-(1→4)-glycosyltransferase (GlgA) encoded by *Rv1212c* (Fig. 6), involved in glycogen and capsular glucan biosynthesis, both α-(1→4)-linked polysaccharides (Sambou et al., 2008). The 6-*O*-methylation of MGLP glucoses was shown to be coordinated by *Rv3030* encoding a putative S-adenosylmethionine (SAM)-dependent methyltransferase (Fig. 6). Inactivation of the *M. smegmatis* homolog (MSMEG2349) caused a substantial decrease in MGLP levels (Stadthagen et al., 2007). The *Rv3037* gene was also proposed to encode a putative SAM-dependent methyltransferase for 3-*O*-methylation of the non-reducing end glucose, although this lacks experimental confirmation (Jackson & Brennan, 2009).

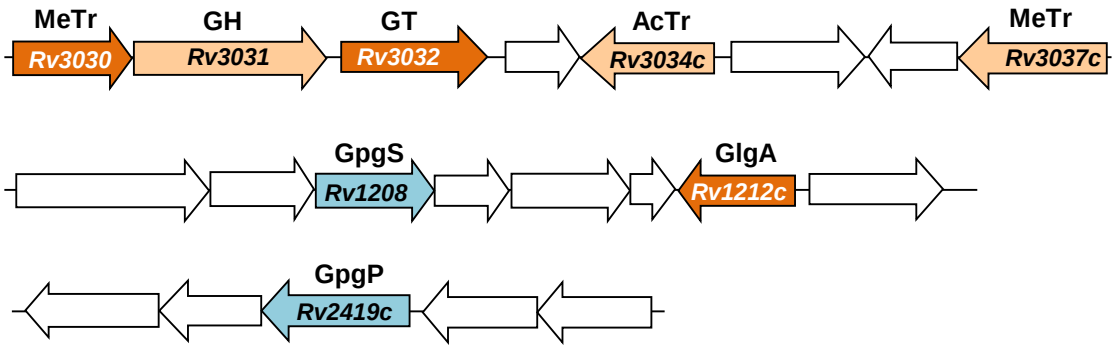

Figure 6 - Genetic clusters proposed to participate in MGLPs biosynthesis in *M. tuberculosis* H37Rv. The genes involved in GG synthesis are shaded blue (see section 1.5.1) and genes for subsequent steps are shaded orange: dark orange, genes whose function have been confirmed; light orange, genes whose function is hypothetical. MeTr, methyltransferase; GH, putative glycoside hydrolase; GT, glucosyltransferase; AcTr, putative acyltransferase; GpgS, glucosyl-3-phosphoglycerate synthase; GlgA, α-(1→4)-glycosyltransferase; GpgP, glucosyl-3-phosphoglycerate phosphatase (adapted from Mendes et al., 2012).

It was recently proposed that the elongation of MGLP may also occur through a newly discovered trehalose synthase-maltokinase-maltosyltransferase (TreS-Mak-GlgE) system (Elbein et al., 2010). This pathway consumes trehalose, a ubiquitous glucose disaccharide essential for mycobacterial growth (De Smet et al., 2000; Murphy et al., 2005). The enzyme TreS converts trehalose (α-D-glucosyl-(1→1)-D–glucose) into maltose (α-D-glucosyl-(1→4)-D-glucose), which is further converted into maltose-1-phosphate (M1P) by a maltokinase (Mak) (Mendes et al., 2010) (Fig. 7). This enzyme is encoded by *Rv0127* in *M. tuberculosis* H37Rv (Fig. 7), which is essential for growth (Sassetti et al., 2003). The Mak from *M. bovis* BCG has been characterized (Mendes et al., 2010). The maltose-1-phosphate formed is, hypothetically, the donor of maltose transferred to MGLP by the maltosyltransferase (GlgE) to elongate the main chain (Kalscheuer et al., 2010). The GlgE is encoded by *Rv1327c* (Fig. 7) and has also been considered essential for *M. tuberculosis* growth (Sassetti et al., 2003; Kalscheuer et al., 2010).

1.5.1 Biosynthesis of glucosylglycerate (GG) in mycobacteria

Glucosylglycerate (α-D-glucopyranosyl-(1→2)-D-glycerate) is a versatile molecule with distinct roles in different organisms. GG accumulates during the adaptation of bacteria and archaea to salt stress (Empadinhas & Da Costa, 2011) but, in some organisms, it can accumulate during nitrogen-limiting conditions (Kollman et al., 1979). In *M. smegmatis*, the concentration of intracellular GG increased in response to nitrogen restriction but its levels decreased sharply when nitrogen sources were fully restored (Behrends et al., 2012). In the absence of a hypoosmotic shock, GG depletion through cell export via pressure-dependent mechanosensitive channels can, in principle, be ruled out (Ruffert et al., 1997). Alternatively, GG can be the substrate of an intracellular glycoside hydrolase activated by nitrogen (Alarico et al, unpublished). Although the knowledge of GG biosynthesis has advanced significantly in the last few years, GG catabolism has not been investigated nor the machinery for hydrolysis and

assimilation of the resulting products. Interestingly, two enzymes with such activity have been recently discovered in thermophilic bacteria (Alarico et al., 2013).

There are three known pathways for GG synthesis: one through a direct condensation of NDP-glucose and D-glycerate by a glucosylglycerate synthase (Ggs) (Fernandes et al., 2007); the second involves a two-step synthesis and hydrolysis of a phosphorylated intermediate, glucosyl-3-phosphoglycerate (GPG), by a glucosyl-3-phosphoglycerate synthase (GpgS) and a glucosyl-3-phosphoglycerate phosphatase (GpgP), respectively (Costa et al., 2006); a third pathway where a putative sucrose phosphorylase produces GG from sucrose and glycerate (Sawangwan et al., 2009). So far, only the two-step pathway has been detected in mycobacteria although an archetypal GpgP is absent from mycobacterial genomes (Empadinhas et al., 2008). In *M. tuberculosis* H37Rv GpgS is encoded by *Rv1208* that was considered essential for growth, hence a promising target for drug development (Sassetti et al., 2003). Two mycobacterial recombinant GpgSs have been characterized (Empadinhas et al., 2008) and the three-dimensional structure of *M. tuberculosis* GpgS has been determined (Pereira et al., 2008).

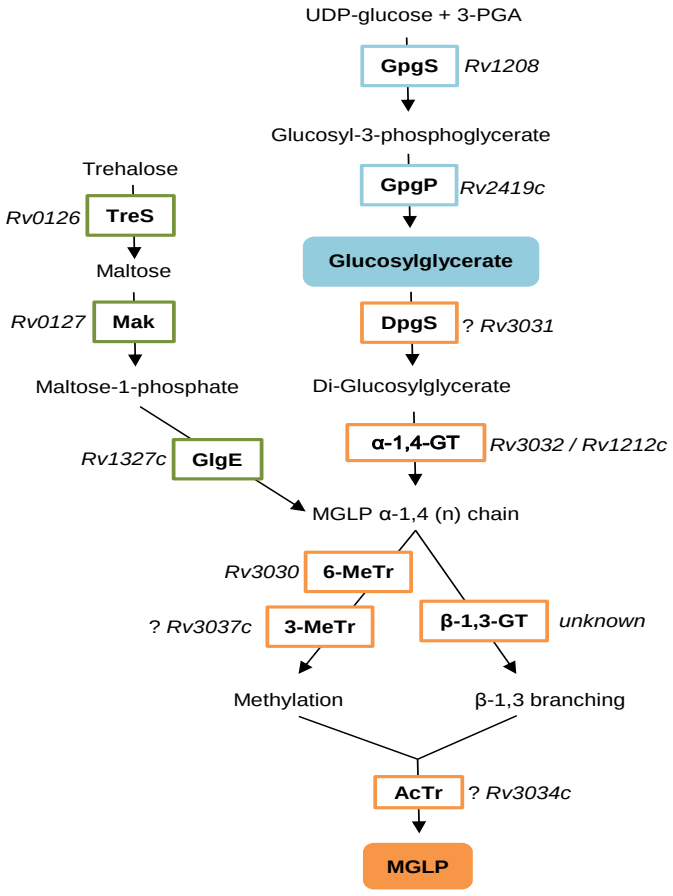

Figure 7 – Model proposed for MGLPs biosynthesis. Blue boxes indicate enzymes involved in GG synthesis, and orange boxes represent enzymes involved in MGLP elongation and maturation. Green boxes represent enzymes involved in TreS-Mak-GlgE pathway. The genes correspond to *M. tuberculosis* H37Rv.
GpgS, glucosyl-3-phosphoglycerate synthase;
GpgP, glucosyl-3-phosphoglycerate phosphatase;
DggS, putative di-glucosylglycerate synthase;
GT, glucosyltransferase;
6-MeTr, methyltransferase;
3-MeTr, putative methyltransferase;
AcTr, putative acyltransferase;
TreS, trehalose synthase;
Mak, maltokinase;
GlgE, maltosyltransferase;
(adapted from Mendes et al., 2012).

A new type of GpgP was recently purified from *M. vanbaalenii* extracts and the genuine function assigned to the corresponding gene (*Rv2419c*), which was incorrectly annotated as a putative phosphoglycerate mutase (PGM) in mycobacterial genomes (Mendes et al., 2011). The *M. tuberculosis* GpgP (mGpgP), which is not a sequence homolog of known GpgPs, was recombinantly produced and biochemically characterized (Mendes et al., 2011). This enzyme was highly specific for GPG and represents the 2nd family with this substrate specificity (Empadinhas & Da Costa, 2011). To understand the catalytic mechanism and active site architecture of this unusual enzyme, a 2Å resolution x-ray native dataset was recently collected from suitable crystals for three-dimensional structure determination (unpublished results).

1.6 Glycoside Hydrolases

Carbohydrates are ubiquitous organic molecules with essential functions in nature such as energy storage, structural components of cell walls and biological mediation of intra- and intercellular communication, cell differentiation and division, viral and microbial infection, to name a few (Hancock et al., 2007; Okuyama, 2011).

Glycoside hydrolases (GHs) are crucial enzymes for carbohydrate metabolism as they catalyse the hydrolysis of glycosidic linkages of glycosides, oligosaccharides, polysaccharides, glycolipids, glycoproteins and glycoconjugates (Hancock et al., 2007; Okuyama, 2011). The hydrolysis can occur through two major mechanisms: inversion or retention of anomeric configuration of the substrate during the reaction (Sinnott, 1990). These mechanisms depend on the spatial position of catalytic residues and allow GHs to be classified as “inverting” or “retaining” enzymes (www.cazy.org).

Since 1984, the IUBMB nomenclature (International Union of Biochemistry and Molecular Biology Enzyme nomenclature) (www.expasy.org/enzyme) of glycosyl hydrolases (EC 3.2.1.-) is based on the type of reaction mechanism and on substrate-specificity. However, structural features were not considered in this classification, and a new one based on amino acid sequence similarities was proposed, since there is a direct relationship between sequence and

folding similarities that reflect the structural features of enzymes better than their substrate specificity alone (Henrissat, 1991; Cantarel et al., 2009). Since protein three-dimensional structures are more highly conserved than their sequence, the GH families were grouped into "clans" (Table 2) (Henrissat & Bairoch, 1996) as they share common ancestry and similarities in the most important functional characteristics, namely residues in the active center, the anomeric configuration of cleavage and the molecular mechanism of the reaction (Naumoff, 2011). Currently, there are 132 GH families that are continuously updated on the Carbohydrate-Active Enzymes database (CAZy) (www.cazy.org) (Cantarel et al., 2009).

Table 2: Glycosyl Hydrolase Clans

CLAN	GH FAMILIES
GH-A	1, 2, 5, 10, 17, 26, 30, 35, 39, 42, 50, 51, 53, 59, 72, 79, 76, 113, 128
GH-B	7, 16
GH-C	11, 12
GH-D	27, 31, 36
GH-E	33, 34, 83, 93
GH-F	43, 62
GH-G	37, 63
GH-H	13, 70, 77
GH-I	24, 46, 80
GH-J	32, 68
GH-K	18, 20, 85
GH-L	15, 65, 125
GH-M	8, 48
GH-N	28, 49

Clan GH-G of glycoside hydrolases is composed of families GH37 and GH63. In this clan, the enzymes share a common three-dimensional structure in $(\alpha/\alpha)_6$ barrel fold (Hancock & Columbia, 2007). Moreover, the enzymes in these families possess an inverting mechanism of hydrolysis, which occurs through a single displacement mechanism (Okuyama, 2011). Family 63 integrates α-glucosidases (EC 3.2.1.106; EC 3.2.1.20), α-1,3-glucosidase (EC 3.2.1.84) and others with unprobed specificities, which in general hydrolyze α-glucose moieties, usually in the non-reducing end (Okuyama, 2011). The recently discovered mannosylglycerate hydrolases

(MgHs) from *Thermus thermophilus* and *Rubrobacter radiotolerans*, reported to catalyze an unprecedented reaction by specifically hydrolyzing α-mannosylglycerate (or α-glucosylglycerate) to mannose (or glucose) and glycerate, were included into family GH63 (Alarico et al., 2013).

While the contribution of genomics into the understanding of mycobacterial physiology is indisputable, annotation of mycobacterial genes based on related sequences from distant taxa is far from being a reliable approach to validate function (Mendes et al., 2011). A striking example concerns the *M. tuberculosis* genome that was sequenced 15 years ago (Cole et al., 1998) but in which over half of the ~4000 predicted genes still wait to be associated to authentic functions (http://tuberculist.epfl.ch/). Therefore, functional characterization of new enzyme activities is crucial from a fundamental point of view but also to establish the foundations upon which new and better strategies to fight mycobacterial diseases may be built.

CHAPTER 2 - MATERIALS AND METHODS

SECTION I: Identification and biochemical characterization of a glucosylglycerate hydrolase (GgH) from *Mycobacterium hassiacum*

2.1 Bacterial growth conditions and DNA extraction

Mycobacterium hassiacum DSM 44199 was obtained from the Deutsche Sammlung von Mikroorganismen und Zellkulturen (Germany) and grown in rich GPHF solid medium (DSMZ 553) supplemented with 2% Tween 80 (2 $g.L^{-1}$) at 50ºC for 48 h (Annex I, Section 1). The genomic DNA was isolated with a protocol adapted from Nielsen and collaborators (1995) (Annex I, Section 2).

To grow *M. hassiacum* under nitrogen-limited conditions, which stimulate the accumulation of GG, cultures were performed in a modified Middlebrook 7H9 medium where the nitrogen source was 1 mM of ammonium sulphate ($(NH_4)_2SO_4$), ferric ammonium citrate was replaced by ferric citrate, and where sodium citrate, L-glutamic acid and copper sulfate were removed (Annex I, Section 3). Growth was carried out during one week at 50ºC in metal-capped flasks containing 250 ml of medium, with continuous aeration, stirred at 150 rpm and turbidity was monitored at 610 nm. Culture aliquots (10 mL) were harvested at appropriate times. The nitrogen shock was performed with the addition of $(NH_4)_2SO_4$ (10 mM) to one culture but not to a parallel culture, which served as control (Table 3).

Table 3: Growth conditions at 50ºC

SAMPLING CONDITIONS	GROWTH - OD_{610nm} [a]	
	A	B (control)
Condition 1 (exponential growth)	± 1.2	± 1.1
Condition 2 (Before $(NH_4)_2SO_4$ addition)	± 2.2 [b]	± 2.4
Condition 3 (24h after $(NH_4)_2SO_4$ addition)	± 2.6	± 2.3

a) Since above OD_{610nm}=2.0, *M. hassiacum* cells have a tendency to aggregate hampering accurate measurement of turbidity, optical density (OD) values were approximate.

b) Nitrogen shock (10 mM $(NH_4)_2SO_4$)

2.2 Identification of glucosylglycerate hydrolase (GgH) and phylogenetic analysis

The glucosylglycerate hydrolase gene (*ggH*) was identified in mycobacterial genomes by BLAST searches at the National Center for Biotechnology Information database (NCBI, http://blast.ncbi.nlm.nih.gov/Blast.cgi) with amino acid sequences of MgHs from *Thermus thermophilus* HB27 and *Rubrobacter radiotolerans* RSPS-4, recently reported to hydrolyse the sugar-glycerate osmolytes, mannosylglycerate and glucosylglycerate (Alarico et al., 2013). The amino acid sequence of GgH (ZP_11162064) from *Mycobacterium hassiacum* DSM 44199 was retrieved from the genome sequence (Tiago et al., 2012) and used for the alignments performed with the BioEdit Sequence Alignment Editor and the phylogenetic tree generated with MEGA5.2 (Tamura et al., 2011)

2.3 Amplification, cloning and functional overexpression of *ggH*

2.3.1 PCR amplification

The *ggH* gene was amplified from chromosomal DNA of *M. hassiacum* with forward primer 5'-AATTGAGT**CATATG**CCGCACGACCCGAGTT designed to include an *Nde*I restriction site (bold), and the reverse primer 5'-CAT**AAGCTT**GCCCAGCCAGTCGAGCAC that includes a *Hind*III site (bold). The stop codon was removed from the reverse primer, allowing the translation of a C-terminal 6×His-tag from the expression vector pET30a (Novagen). PCR amplification was carried out with proofreading KOD Hot Start DNA polymerase (Novagen), according to the manufacturer's instructions with the following conditions: pre-incubation step at 95ºC for 2 min, followed by 30 cycles of denaturation at 95ºC for 30 s, annealing temperature at 55ºC for 30 s and primer extension at 70ºC for 50 s. The extension step in the last cycle was prolonged for 10 min. The PCR product was visualised after agarose gel electrophoresis (Annex I, Section 4) and purified with JETquick Gel Extraction Spin Kit (Genomed), according to the suppliers' instructions.

2.3.2 Cloning and transformation of *E. coli* BL21

The 1341 bp *ggh* gene and the cloning/expression vector pET30a (Novagen) were digested with restriction enzymes *Nde*I and *Hind*III (Takara) at 37ºC for 1 h. Digested fragments were visualized in agarose gel electrophoresis and purified as described above followed by cloning into pET30a vector with the Speddy Ligase Kit (NYZTech). Ligation was performed during 20 min at room temperature. Recombinant plasmids were used to transform *E. coli* BL21 competent cells as follows: 10 µL of plasmid were added to 100 µl of competent cells (Annex I, Section 5) and incubated on ice for 20 min, followed by a 42ºC heat shock in a pre-heated water bath for 45 s. 500 µL of LB medium (Annex I, Section 6) with 1% of salt solution (Annex I, Section 7) were added to the cells and incubated at 37ºC for 1 h. Aliquots of 300 µl of the culture were transferred into LB agar medium containing kanamycin (30 µg/mL) and incubated at 37ºC for about 16 h for selection. Resistant colonies were cultured in metal capped-tubes containing 5 mL of LB medium and kanamycin (30 µg/mL), in a shaker incubator (150 rpm) at 37ºC. Plasmid extraction was performed using ZR plasmid miniprep™-classic kit (Zymo Research), according to the suppliers' instructions. To confirm the positive clones, plasmids were digested with *Nde*I and *Hind*III restriction enzyme and visualized in agarose gel electrophoresis.

2.3.3 Overexpression of the *ggH* gene

Escherichia coli BL21 cells containing the recombinant plasmidwere grown in LB liquid medium (2 L) containing kanamycin (30 µg/mL) to mid-exponential phase (OD_{610nm}=0.8) with continuous aeration at 37ºC. Expression was induced with 0.5 mM isopropyl β-D-1-thiogalactopyranoside (IPTG) and growth was allowed to proceed for 24 h at 25ºC and stirred at 150 rpm. Cells were harvested by centrifugation (9000 rpm, 10 min, 4ºC), suspended in Buffer A (Annex I, Section 8) containing 5 mM $MgCl_2$ and 2 mg/ml DNAseI, and disrupted with a sonicator followed by centrifugation (15000 rpm, 15 min, 4ºC) to remove cell debris.

2.4 Purification of the recombinant GgH

The His-tagged recombinant GgH from *M. hassiacum* was purified in a fast protein liquid chromatography (FPLC) system, with a Ni-Sepharose column (HisPrep™ FF16/10, GE Healthcare). The column was equilibrated with Buffer A (Annex I, Section 8). The crude protein extract (section 2.3.3) was filtered through a 0.45 µm cellulose filter before injection. Elution of the target His-tagged protein was carried out with Buffer B (Annex I, Section 9). Fractions (4 mL) were collected and the purity determined by SDS-PAGE (Annex I, Section 10). The purest fractions were pooled, concentrated with 30 kDa cut-off centricons (Amicon) and equilibrated with 20 mM sodium phosphate buffer at pH 7.0 containing 200 mM NaCl. The protein content was quantified by the Bradford protein assay (BioRad) and the activity of the enzyme examined by thin-layer chromatography (TLC) (Silica Gel 60, Merck) using a solvent system composed of chloroform/methanol/acetic acid/water (30:50:8:4, v/v/v/v). TLC plate was stained with α-naphthol/sulphuric acid reagent (Annex I, Section 11) at 120ºC for 10 min.

2.4.1 Determination of the molecular mass of the recombinant GgH

The molecular mass and extent of oligomerization of recombinant GgH was estimated by gel filtration chromatography after loading the purified GgH onto a Superdex 200 column (HiLoad 16/600 Superdex 200, GE Healthcare), according to Gel Filtration Calibration Kit instructions (GE Healthcare). The column was pre-equilibrated with 20 mM sodium phosphate buffer, pH 7.0 containing 200 mM NaCl and the following molecular mass standards were used: conalbumin (75 kDa), carbonic anhydrase (29 kDa), ribonuclease A (13.7 kDa), ovalbumin (44 kDa) and aprotinin (6.5 kDa). Blue dextran 2000 was used to determine the void volume. These experiments were performed in duplicate.

2.5 Enzyme assays and substrate specificity

The substrate specificity of GgH was tested in 50 µL mixtures containing pure enzyme (10 µg) and 10 mM of each the following substrates: mannosylglycerate (MG), glucosylglycerate, α,α-trehalose, sucrose, isomaltose and glucosylglucosylglycerate (GGG). The reactions were carried out with 25 mM sodium phosphate buffer at pH 5.7, 5 mM $MgCl_2$ and 100 mM KCl at 42ºC for 1 h. Each reaction was spotted onto a TLC plate and developed as described above.

Quantification of the glucose released from glucosylglycerate, α,α-trehalose, sucrose, isomaltose and glucosylglucosylglycerate by GgH was carried out with the glucose oxidase (GO) assay kit (Sigma-Aldrich), according to the suppliers' instructions. The reactions were performed in duplicate under the conditions above and stopped after 8 or 30 min on ethanol-ice. Synthetic compounds used as general glycosidase substrates (4-nitrophenyl-α-D-glucopyranoside and 4-nitrophenyl-α-D-glucopyranoside) were also tested as possible substrates for the GgH using a spectrophotometric method that followed the increase in absorbance at 410 nm. Reactions without the enzyme were used as negative controls.

2.6 Biochemical and kinetic characterization of GgH

Temperature and pH profiles, dependence of cations, effect of salt and thermal stability as well as kinetic parameters were determined. Reactions (50 µL) were performed with the appropriate buffer and cations, 6.4 µg of GgH and 10 mM GG incubated at different times (2, 4, 6, 8 min) and stopped by cooling on ethanol-ice. The release of glucose from GG was quantified as mentioned above and the enzymatic assays were performed in triplicate.

The temperature profile was determined between 25ºC and 60ºC in mixtures with 16 mM sodium phosphate buffer at pH 5.7 (reference buffer), 5 mM $MgCl_2$ and 100 mM KCl. Thermal stability was determined by incubating the enzyme in reference buffer containing 100 mM KCl at 37, 42 and 50ºC. Samples were cooled at different times (minutes to hours) and the GgH residual activity was examined under optimal reaction conditions at 42ºC.

The effect of pH was tested using the following buffers: 16 mM or 25 mM acetate buffer (pH 4.0 - 6.5); 25 mM citrate-phosphate buffer (pH 2.6 - 5.0); 25 mM MES buffer (pH 5.5 - 6.5); 16 mM or 25 mM sodium phosphate buffer (pH 5.7 - 7.0) (additionally, concentrations of 5, 8, 12, and 20 mM at pH 5.7 were also tested). Reaction mixtures contained 5 mM of $MgCl_2$ and 100 mM of KCl and were incubated at 42ºC. The buffer pH values (measured at 25ºC) at 42ºC were adjusted using the conversion factor ($\Delta pKa/\Delta T$ [°C]) of 0.002 for acetate buffer, -0.011 for MES buffer and -0.0028 for sodium phosphate buffer (Good et al., 1966).

The effect of cations was examined in reactions with 5 mM of the chloride salts of Mg^{2+}, Mn^{2+}, Co^{2+}, Ca^{2+}, Fe^{2+}, Zn^{2+} and Cu^{2+}. Reactions were carried out in reference buffer containing 100 mM of KCl at 42ºC and compared with reactions without cations or with 5 mM of ethylenediaminetetraacetic acid (EDTA). Moreover, 2, 5 and 10 mM of $MgCl_2$ and $CaCl_2$ were also tested in mixtures with reference buffer containing 100 mM of KCl, incubated at 42ºC. The presence of KCl was essential to stabilize the recombinant GgH. The effect of KCl on enzyme activity was tested by addition of 15, 40, 100, 150 or 200 mM to reference buffer containing 5 mM of $MgCl_2$.

Kinetic parameters were determined from the release of glucose, as described above, after incubation (2, 4, 6 and 8 min) of reaction mixtures with 6.4 µg of GgH and increasing concentrations of GG (1 - 24 mM), and under optimum conditions of the enzyme. K_m and V_{max} were determined with GraphPad Prism (version 5.00) Software, San Diego, CA, USA (http://www.graphpad.com), where Michaelis-Menten equation was used (nonlinear regression). All experiments were performed in duplicate.

2.7 Determination of intracellular levels of GG in *M. hassiacum* under nitrogen-limited conditions

Samples collected in section 2.1 (Table 3) were used to extract intracellular organic solutes by the addition of 80%ethanol and boiling for 10 min. The ethanol was evaporated at 60ºC and 100 µL of ultrapure sterile water were added to the remaining soluble extract and stored at -80ºC. After lyophilisation, extracts were rehydrated with 240 µL of water. Samples were homogenized with ½ volume of chloroform (to remove lipids) following by centrifugation (14000 rpm, 5 min). The aqueous phase containing soluble organic solutes was collected (10 µL) and visualized by TLC as described above. The amounts of GG accumulated in the conditions tested were quantified using the recombinant GgH (20 µg) in reaction mixtures containing reference buffer, 5 mM of $MgCl_2$ and 100 mM of KCl. Reactions were incubated overnight at 42ºC to ensure total conversion of GG into glucose, which was then quantified using the Glucose (GO) assay kit. At the same time, it was used the recombinant MgH (20 µg) from *R. radiotolerans* (Alarico et al., 2013) in reaction mixtures containing acetate buffer 50 mM pH 4.0 and were incubated 3 h at 55ºC to ensure again total conversion of GG into glucose and was quantified with the same kit mentioned above.

To determine the dry weight of cells, cell suspensions (1 mL) were centrifuged and the pellets were dried for 2 h at 65ºC.

SECTION II: *Mycobacterium hassiacum*, a rare source of heat-stable proteins

To test and validate the higher thermal stability of proteins from *M. hassiacum* we studied the thermal stability of the *M. hassicum* GpgS and compared its profile with homologous enzymes from the mesophilic *M. smegmatis* and *M. bovis* BCG (Empadinhas et al., 2008).

2.1 Cloning and expression of *M. hassiacum gpgS* and purification of GpgS

The *gpgS* gene from *M. hassiacum* was amplified as described above and cloned into expression vector pET30a. The construct was sequenced (LGC Genomics) and transformed into *E. coli* BL21. Expression was induced with 0.5 mM IPTG and growth allowed to proceed for additional 4 h at 37ºC. The recombinant His-tagged GpgS was purified with a Ni-Sepharose high-performance column (His–Prep FF 16/10) (Alarico et al. personal communication).

2.2 Thermal stability of *M. hassiacum* GpgS

Thermal stability was determined by incubating recombinant GpgS aliquots (30 µl of a solution of 1 $mg.ml^{-1}$) in 25 mM Bis-tris propane (BTP) buffer, pH 7.0 at 37 and 50°C. Aliquots were withdrawn at defined times (up to 5 days) and examined for residual activity under the following conditions: reaction mixtures with a final volume of 50 µL containing 25 mM BTP buffer, 2.5 mM UDP-glucose, 2.5 mM 3-PGA, 20 mM $MgCl_2$, 1 µg of GpgS and 5 µg of MpgP (mannosyl-3-phosphoglycerate phosphatase) from *Thermus thermophilus* to specifically dephosphorylate GPG (glucosyl-3-phosphoglycerate) (Empadinhas et al., 2003). The quantification of free phosphate was performed by the Ames protocol (Ames, 1966). Reaction mixtures were incubated at 37ºC and stopped at different times by cooling on ethanol-ice. The assays were performed in triplicate and reactions without enzymes, only with MpgP or only in presence of one of the substrates (UDP-glucose or 3-PGA) were used as controls.

CHAPTER 3 - RESULTS

SECTION I: Identification and biochemical characterization of a glucosylglycerate hydrolase (GgH) from *Mycobacterium hassiacum*

3.1 Sequence analysis and phylogenetic tree

The 1341 bp *ggh* gene from *M. hassiacum* DSM 44199 encodes a 447 amino acid polypeptide with a calculated molecular mass of 51.2 kDa, kDa, with a calculated isoelectric point of 5.88. BLAST analyses with amino acid sequence of GgH revealed the closest homologs in *M. fortuitum* DSM 46621 (89%), in *M. vanbaalenii* PYR-1 (87%), in *M. phlei* RIVM601174 (88%), in *M. smegmatis* mc²155 (88%), and more distantly related homologues in *Thermus thermophilus* HB27 (36%) and *Rubrobacter radiotolerans* (34%). Since the *M. hassiacum* GgH had motifs of glycoside hydrolase family 63 (GH63) it will be included into this family in the CAZy database.

The phylogenetic tree based on GgH sequences revealed that GgH homologues are absent from slowly-growing mycobacteria (except *M. tusciae*) (Fig. 8). The cluster with the MgHs from *T. thermophilus* and *R. radiotolerans* was clearly separated from GgHs indicating a more distant relationship at the phylogenetic level.

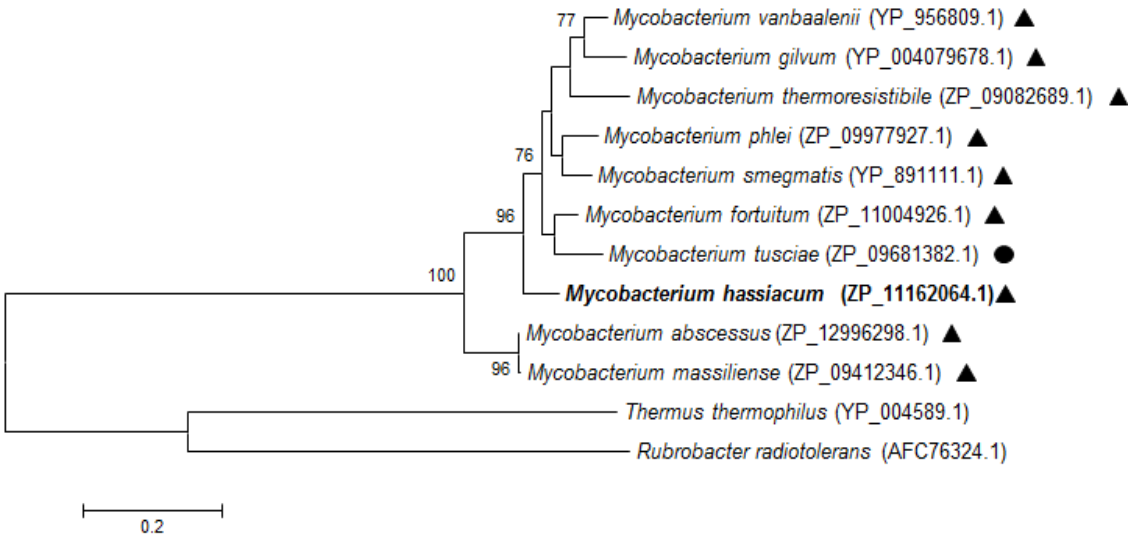

Figure 8 - Phylogenetic analysis based on the amino acid GgH sequence from *M. hassiacum* and homologues. Shaded triangles indicate rapidly-growing species and shaded circle indicates slowly-growing mycobacteria. The significance of the branching order was evaluated by bootstrap analysis of 1000 computer-generated trees. The bootstrap values are indicated. Bar, 0.2 change/site. GenPept accession numbers are in parenthesis.

3.2 Purification and molecular mass of the *M. hassiacum* recombinant GgH

The recombinant His-tagged bioactive GgH was purified to homogeneity in one step with a Ni-Sepharose column (Fig. 9 and 10).The enzyme behaved as a dimeric protein in solution, with a mass of 108.9±2.6 kDa, as determined by size-exclusion chromatography.

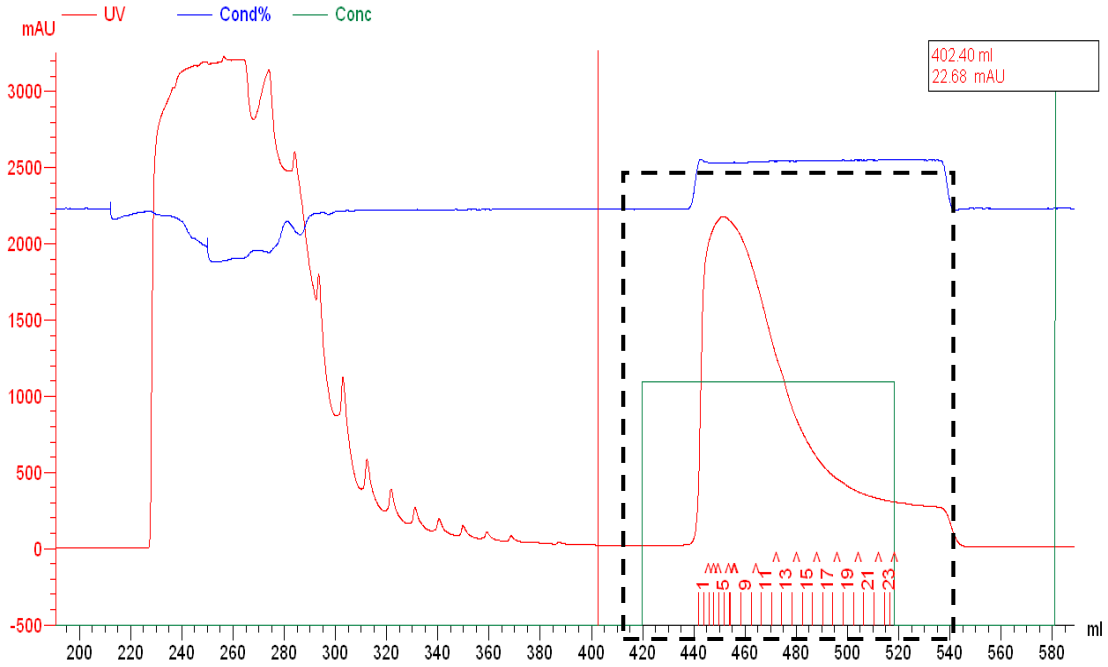

Figure 9 - FPLC chromatogram obtained during recombinant GgH purification with a Ni-Sepharose column. Dashed area represents eluted tagged protein content with 40% of elution buffer.

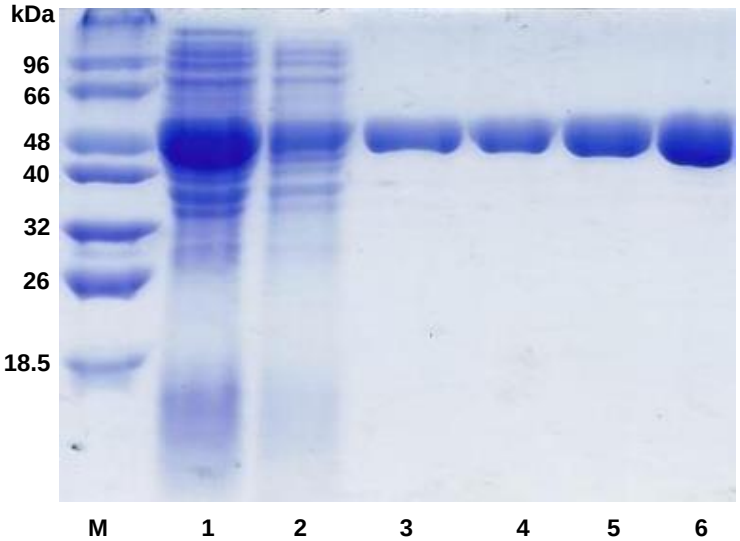

Figure 10 – SDS-PAGE gel of the purification steps of recombinant GgH from *M. hassiacum*. **Lane 1:** soluble fraction of cell-free extract before loading the column; **lanes 2 - 6:** fractions 3, 7, 9, 11 and 13 (chromatogram) collected after elution (Fig. 9); **lane M:** molecular mass marker.

3.3 Substrate specificity of GgH

Among the substrates tested (see section 2.5) the recombinant GgH was only able to hydrolyse GG into glucose and glycerate, analysed either by TLC (Fig. 11) or by glucose quantification as described in the Methods section (section 2.5). Furthermore, trace activity was detected in assays with the related mannosylglycerate (MG) after 1 h incubation at 42ºC.

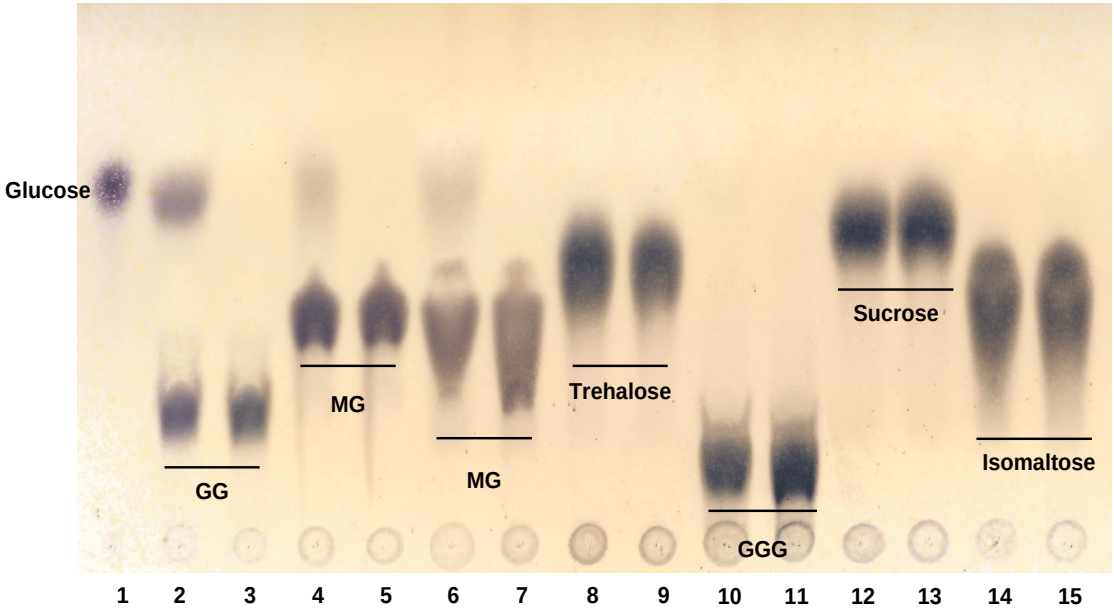

Figure 11 - TLC analysis of GgH substrate specificity with conditions described in section 2.5 of Materials and Methods. **Lane 1:** Glucose standard; **Even lanes (2 to 14)**, reactions with GgH; **Odd lanes (3 to 15)**, control reactions without enzyme. All but reactions in lanes 4 and 5 contained 100 mM KCL.

3.4 Biochemical characterization of GgH

The activity of GgH was almost undetectable below 25ºC and above 55ºC, with maximum at 42ºC (Fig. 12). The enzyme was maximally active between pH 5.5-6.0 with maximal activity at 5.7 (sodium phosphate buffer) (Fig. 13). Citrate-phosphate buffer inhibited GgH activity.

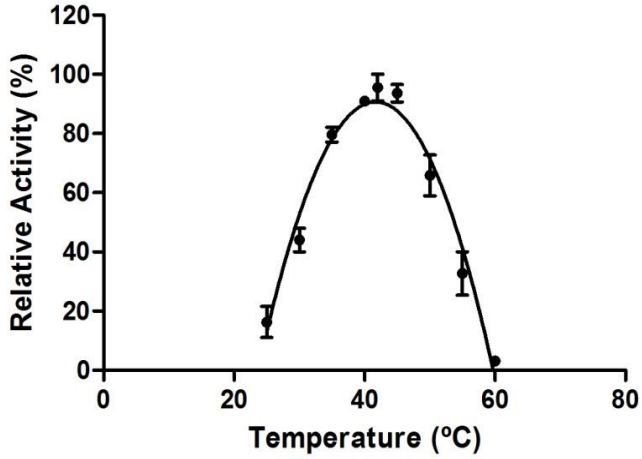

Figure 12 - Temperature profile for activity of the recombinant GgH.

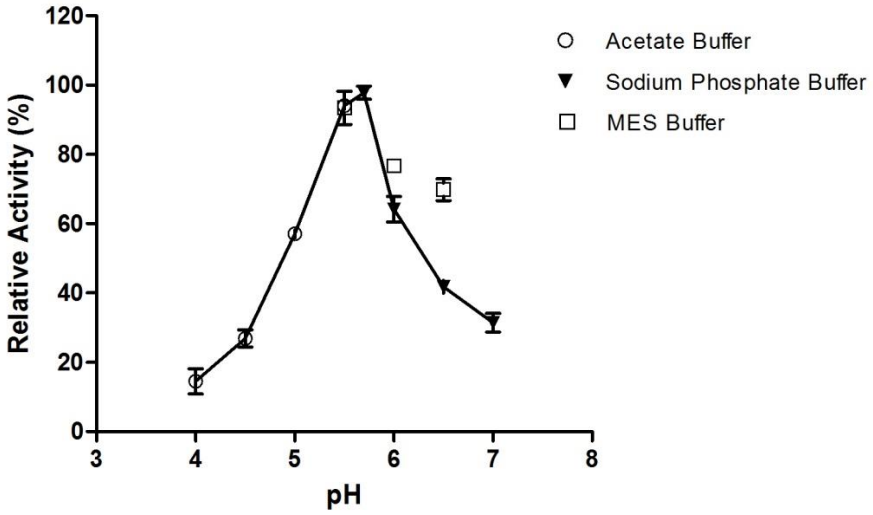

Figure 13 - pH dependence of GgH activity.

Although GgH activity was not dependent on cations, Mg^{2+} ions stimulated catalysis and maximal stimulation was achieved with 5 mM (Figs. 14 and 15). On the other hand, Mn^{2+}, Co^{2+}, Cu^{2+}, Fe^{2+}, Zn^{2+} ions were inhibitory whereas Ca^{2+} did not affect GgH activity (Figs. 14 and 15). KCl also stimulated GgH activity with maximal stimulation achieved with 100 mM (Fig. 16). The GgH was unstable at 4ºC and gradually precipitated. KCl significantly stabilised the enzyme at concentrations of 100-200 mM.

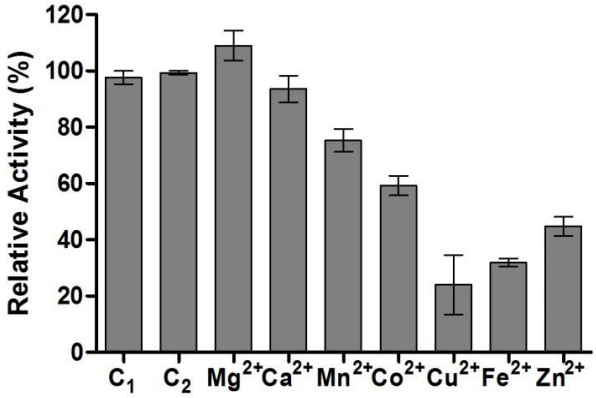

Figure 14 - Cations dependence of GgH activity.

C_1: reaction without cations; **C_2:** reaction in the presence of EDTA.

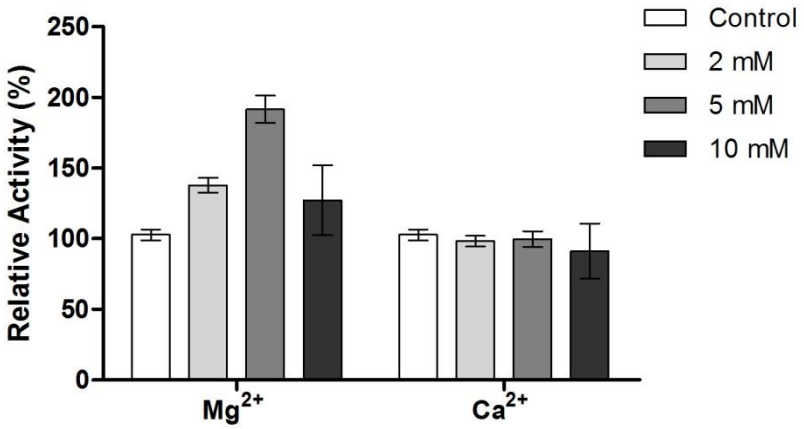

Figure 15 - GgH activity in the presence of different concentrations of Mg^{2+}or Ca^{2+}.

Control reaction was performed without cations.

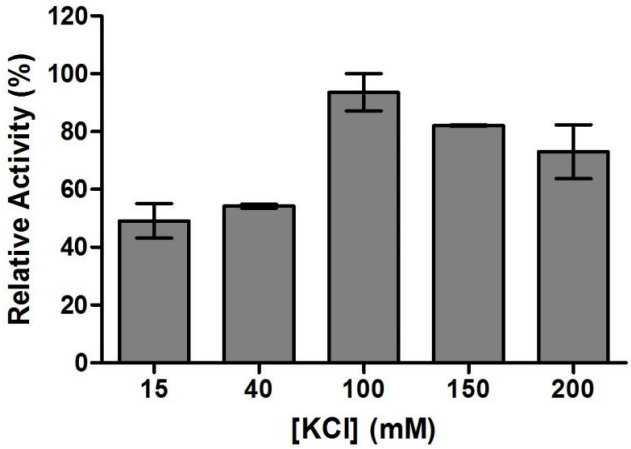

Figure 16 - Effect of KCl in GgH activity.

Half-life values for inactivation of GgH at 37, 42 and 50ºC were 63.6±18.0 h, 15.7±1.2 h and 0.4±0.2 h, respectively. At 50°C, the residual activity progressively decreased during the initial 2 h but, after this period, the activity retained 30% of maximum activity for 24 h (Fig. 17).

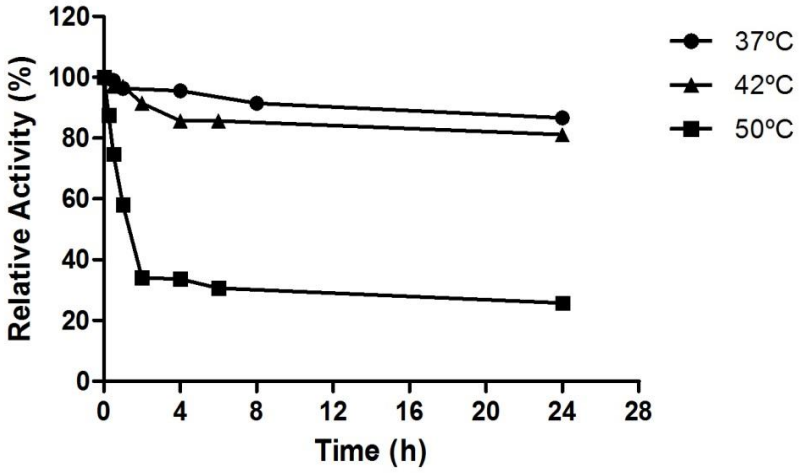

Figure 17 - Thermal stability of GgH at different temperatures.

3.5 Kinetic studies

The *M. hassiacum* GgH exhibited Michaelis-Menten kinetics at 37, 42 and 50ºC with GG tested at concentrations up to 24 mM (Figs. 18-20). Kinetic parameters (V_{max} and K_m) for GgH are indicated in Table 4. The GgH catalytic efficiency (V_{max}/K_m) for GG hydrolysis at the temperatures tested was comparable.

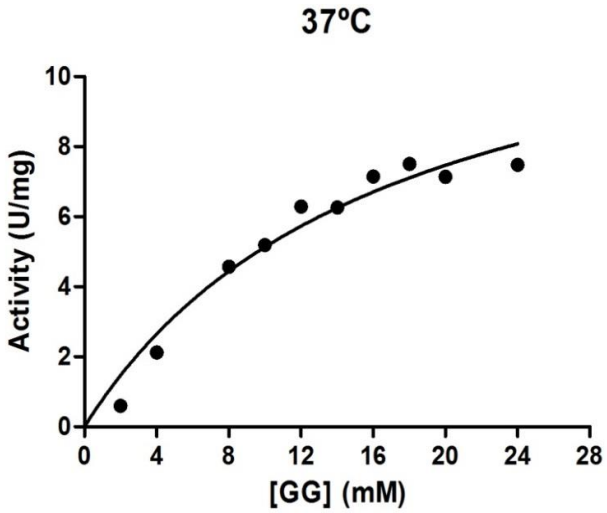

Figure 18 - Effect of GG concentration on GgH activity at 37ºC.

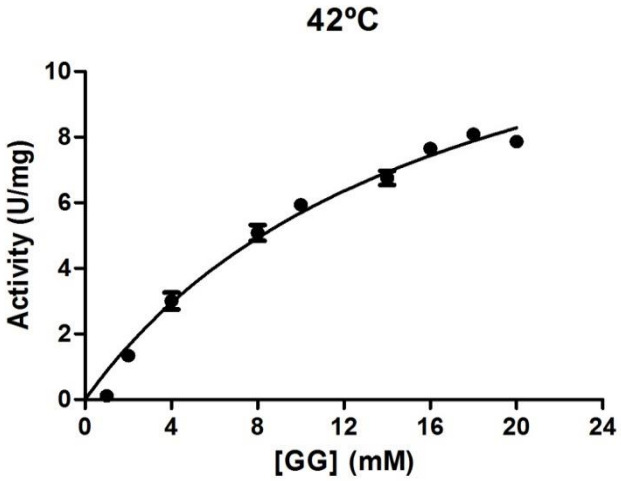

Figure 19 - Effect of GG concentration on GgH activity at 42ºC.

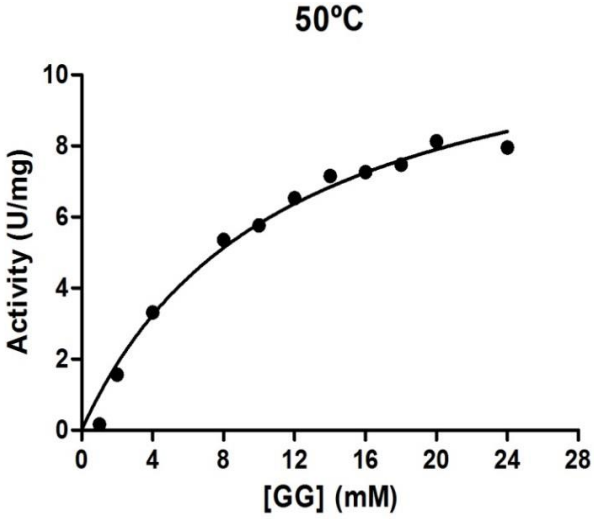

Figure 20 - Effect of GG concentration on GgH activity at 50ºC.

Table 4: Kinetic parameters of recombinant GgH

TEMPERATURE	SUBSTRATE	K_M (mM)	V_{MAX} (µmol/min.mg)	V_{MAX}/K_M RATIO
37ºC	GG	16.69±6.06	13.69±2.60	0.82±0.10
42ºC		16.68±2.99	15.18±1.48	0.91±0.08
50ºC		11.25±2.04	12.34±0.99	1.10±0.08

3.6 Accumulation of GG in *M. hassiacum* under nitrogen-limited conditions

Mycobacterium hassiacum was grown in nitrogen-deficient conditions and the medium was supplemented with 10 mM of $(NH_4)_2SO_4$ at mid-exponential phase of growth (Table 3 of Materials and Methods). The effect of this nitrogen source on GG accumulation was examined either by TLC (Fig. 21) or by quantification of the glucose released, as described in section 2.1 of Materials and Methods (Table 5). *Mycobacterium hassiacum* was also grown in nitrogen-deficient medium (without the $(NH_4)_2SO_4$ shock) and intracellular GG levels examined under the same conditions.

The TLC (Fig. 21) clearly shows that GG content gradually increases as the growth proceeds in nitrogen-limited conditions, and after supplementation with 10 mM $(NH_4)_2SO_4$, a dramatic depletion of the GG levels after 24 h is obvious.

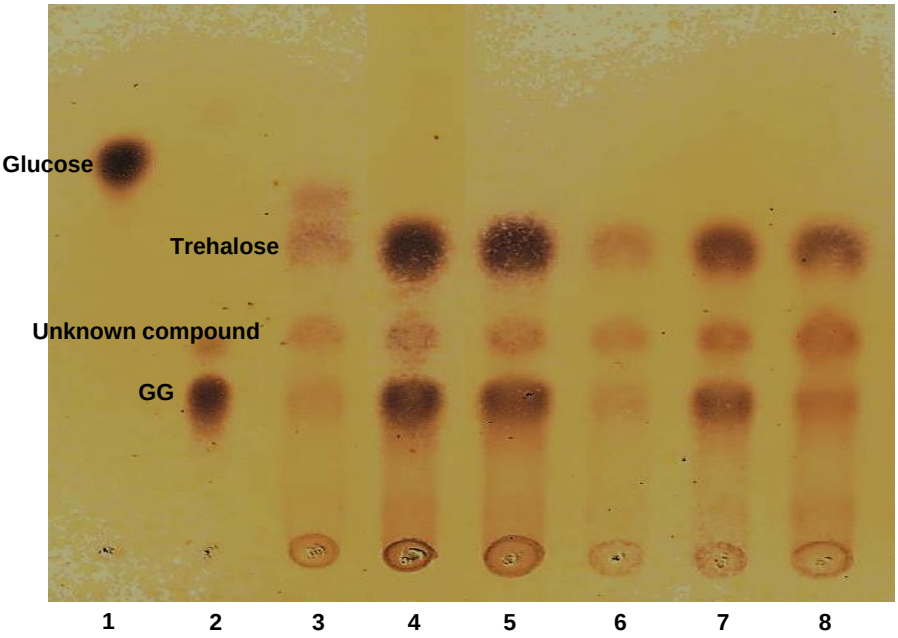

Figure 21 - *M. hassiacum* intracellular organic solutes. Standards: glucose **(lane 1)** and GG (**lane2). Lanes 3-5:** conditions 1 to 3 of growth "B" (Table 3 in Materials and Methods) and **lanes 6-8:** conditions 1 to 3 of growth "A" (Table 3 in Materials and Methods). An unknown spot between GG and trehalose has not been identified.

Aliquots of ethanol extracted solutes were incubated with both GgH (results not shown) and MgH to achieve complete hydrolysis of GG accumulated, as described in the Materials and Methods section, and the reaction products were analysed by TLC (Fig. 22) and by glucose

quantification (Table 5). The TLC indicates that both enzymes seem to completely hydrolyze GG (glucose spots in the upper region of the TLC).

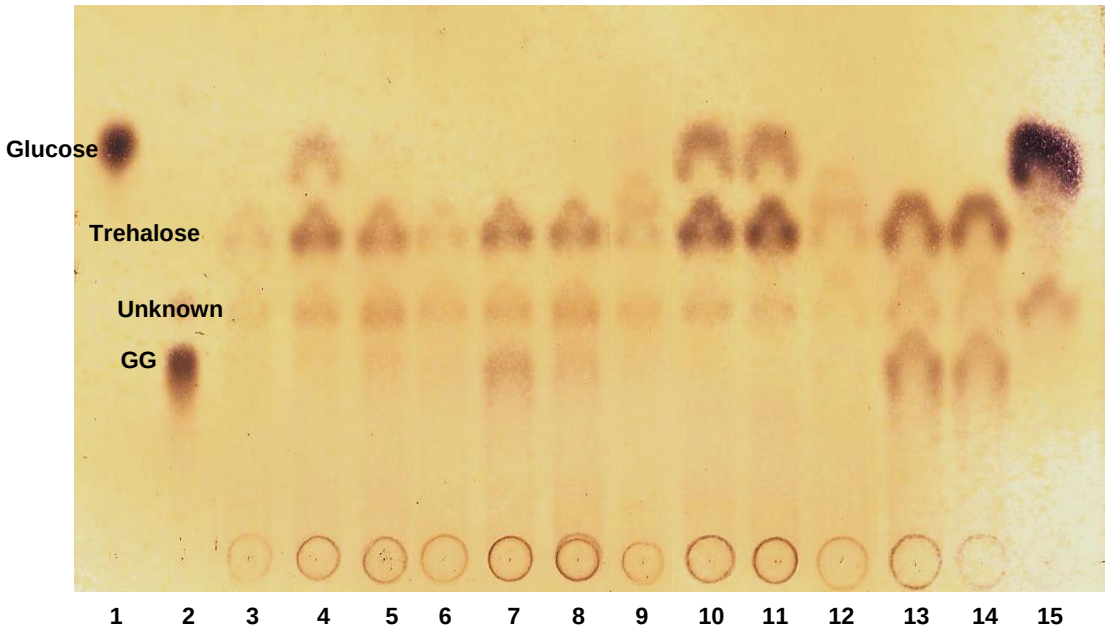

Figure 22 - TLC analysis of GG hydrolysis after incubation of *M. hassiacum* solutes with MgH from *R. radiotolerans*. Standards: glucose **(lane 1)** and GG **(lane2). Lanes 3-5:** reactions of MgH with solutes obtained from growth "A" (Table 3 in Materials and Methods); **lanes 6-8:** control reactions without MgH; **lanes 9-11:** reactions of MgH with solutes obtained from growth "B" (Table 3 in Materials and Methods); **lanes 12-14:** reactions without MgH and solutes from growth "B" (Table 3 in Materials and Methods); **lane 15:** control reaction with synthetic GG. An unknown spot between GG and trehalose has not been identified.

After specific and complete hydrolysis of GG with GgH (results not shown) or with MgH, the 1:1 stoichiometry allows accurate quantification of GG accumulated at all selected phases of *M. hassiacum* growth and of its depletion after the nitrogen upshock. In reactions of quantification (Table 5, Fig. 23), this stoichiometry between glucose released and GG accumulated confirm that GG content is gradually increased in nitrogen-limited conditions and when the medium was supplemented with 10 mM $(NH_4)_2SO_4$ a sharp decrease of the GG levels occurred (Fig. 23).

An attempt to quantify the trehalose accumulated by *M. hassiacum* grown under each of the nutritional conditions and growth phases, based on the specific hydrolysis catalyzed by the α-glucosidase from *T. thermophilus* (Alarico et al., 2008) was unsuccessful, probably because we used an enzyme preparation that was inactive due to long-term storage (>1 year) at -20ºC.

Table 5: Quantification of glucose released from GG with GgH or with MgH

		Glucose released = GG accumulated (µg/mg cell dry weight)	
GROWTH	SAMPLING POINTS (TABLE 3 – METHODS)	GgH	MgH
A	1 (OD=1.2)	6 ± 1	8 ± 3
	2 (OD=2.2)*	43 ± 1	41 ± 2
	3 (OD=2.6)	9 ± 3	2 ± 1
B (without nitrogen shock)	1 (OD=1.1)	7 ± 2	5 ± 2
	2 (OD=2.4)	43 ± 1	41 ± 2
	3 (OD=2.3)	47 ± 2	48 ± 1

* Nitrogen shock

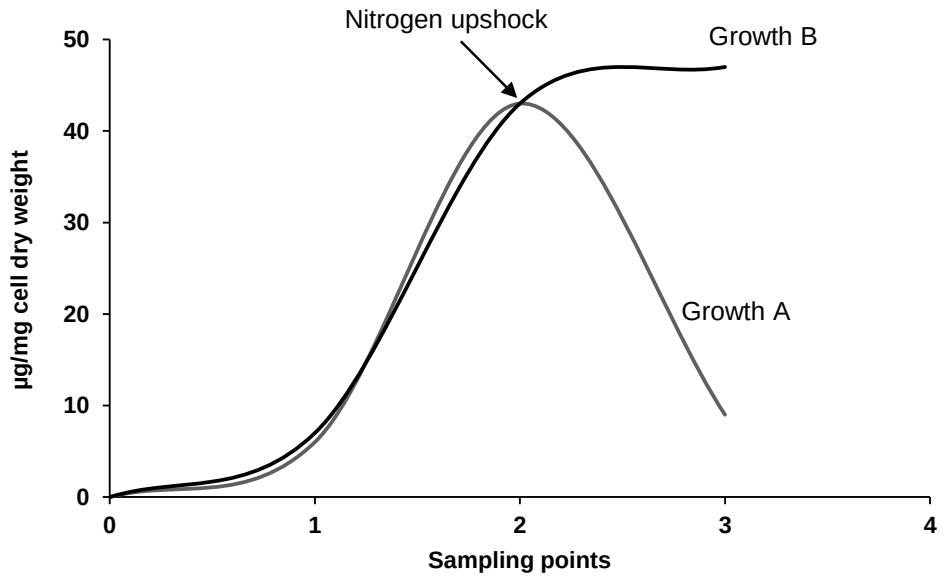

Figure 23 - Levels of GG accumulated at the selected phases of *M. hassiacum* growth curve. Grey line corresponds to growth "A" (Table 3 in Materials and Methods) and black line corresponds to growth "B" (Table 3 in Materials and Methods).

SECTION II: *Mycobacterium hassiacum*, a rare source of heat stable proteins

3.1 Thermal stability of GpgS from *M. hassiacum*

The half-life values for inactivation of the recombinant GpgS from *M. hassiacum* at 37 and 50ºC were 8.25±1.37 and 9.62±2.41 days, respectively (Fig. 24). At both temperatures, the residual activity progressively decreased to about 70% of maximal activity after 4-5 days (Fig. 24).

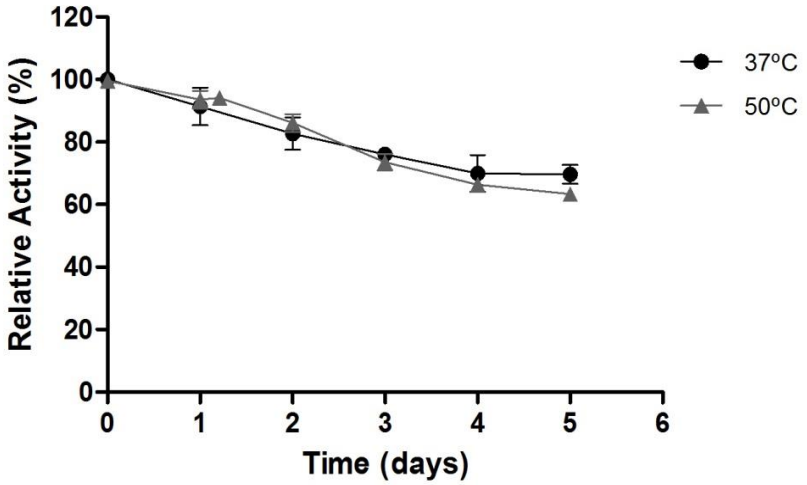

Figure 24 - Thermal stability of GpgS at 37ºC and 50ºC.

The thermal stability of *M. hassiacum* enzymes was also tested in this work and compared with homologous enzymes from other *Mycobacterium* species, in order to confirm its anticipated superior stability (Tiago et al., 2012). The GpgS from *M. hassiacum* has significantly higher thermal stability than GpgS from *M. smegmatis* and *M. bovis* BCG, since this enzyme from *M. hassiacum* displays a half-life time of several days at all temperatures tested, while the GpgSs from mesophilic mycobacteria have half-life values of hours only (Table 6).

Table 6: Thermal stability of three mycobacterial GpgSs

Mycobacterium SPECIES	HALF-LIFE VALUES	
	37ºC	50ºC
Mycobacterium hassiacum	8.25±1.37 days	9.62±2.41 days
Mycobacterium bovis BCG (Empadinhas et al., 2008)	12.42±1.24 h	n.d.
Mycobacterium smegmatis (Empadinhas et al., 2008)	7.28±0.39 h	n.d.

This high thermal stability of enzymes from *M. hassiacum* may be associated with the fact that this bacterium is the most thermophilic species within this genus and is capable to grow at high temperatures (maximum growth temperature of 65ºC) (Alarico et al, unpublished results), which is an important tool for enzyme functional studies and protein crystallography.

CHAPTER 4 - DISCUSSION

The growing number of atypical diseases caused by different species of nontuberculous mycobacteria (NTM) demands an intensification in research to probe their particular characteristics and try to understand the distinctive ecological, physiological and metabolic traits, including the genetic and enzymatic resources that allow them a wide spectrum of environmental adaptation, metabolic versatility and ultimately, infection of the human host (Falkinham, 2009). One of such characteristics is their unique thick cell wall that is one of the factors underlying their adaptive success (Kaur et al., 2009). How mycobacteria erect such an outstanding cell wall has been a focus of research of many decades. Among the cell wall constituents, mycolic acids are major structural players in the biophysical properties of this protective shell. Mycolic acids are assembled from medium-chain fatty acids by complex biosynthetic machinery in the cytoplasmic cell compartment (Takayama et al., 2005).

The synthesis of fatty acids is regulated by polymethylated polysaccharides (PMPSs), soluble structures that are almost exclusively restricted to this group of bacteria and a few closely related taxa (Jackson & Brennan, 2009), whose crucial role in mycobacterial physiology renders them attractive targets for anti-mycobacterial therapies (Mendes et al., 2012). There are two types of PMPSs in mycobacteria, the methylglucose lipopolysaccharides (MGLPs) and the methylmannose polysaccharides (MMPs). MGLPs are present in both rapidly-growing mycobacteria (RGM) and slowly-growing mycobacteria (SGM), but MMPs are mostly restricted to RGM. The pathway for their biosynthesis is largely unknown, although some of the genes and enzymes involved have been recently identified and characterized (Empadinhas et al., 2008; Mendes et al., 2011; Mendes et al., 2012). The reducing end of the MGLP was found to be composed of glucosylglycerate (GG) (Forsberg et al., 1982), which was considered the initial precursor for MGLP biosynthesis.

Glucosylglycerate is synthesized in two steps by an actinobacterial-type GpgS for the first step, which was considered essential for *M. tuberculosis* growth and whose three-dimensional structure has been solved (Pereira et al., 2008). The second step is catalyzed by a GpgP, which represents a new unexpected family of mycobacterial GpgPs (Kamisango et al., 1987;

Empadinhas et al., 2008; Mendes et al., 2011). Although GG is generally accumulated as response to salt stress in a number of organisms, in mycobacteria it was found to accumulate under nitrogen-limiting conditions (Behrends et al., 2012), the same stress condition as it was initially found to accumulate in a strain of *Synechococcus* (Kollman et al., 1979). In some microorganisms of the order *Actinomycetales* there are efflux systems for the rapid release of solutes accumulated during salt stress, to prevent cell lysis during hypoosmotic shocks (Ruffert et al., 1997). However, the existence of these systems in mycobacteria has not been investigated. Moreover, since GG accumulation in mycobacteria is not salt-dependent, the sharp decrease of GG observed during adaptation to nitrogen-rich medium is not likely to be driven by export but instead as the result of enzymatic degradation, as is the case for some thermophilic bacteria (Alarico et al., 2013).

Although the recently identified hydrolases of the glycoside hydrolase GH63 family are very specific for mannosylglycerate (MG), the solute accumulated in the host thermophilic bacteria, they can also hydrolyze GG with comparable catalytic efficiency. Thus, we decided to probe mycobacterial genomes for a similar hydrolase and we selected the thermophilic species *Mycobacterium hassiacum* as model and source of the gene for recombinant protein production.

This organism's genome had been recently sequenced for its inherently stable proteins, suitable for functional and structural studies (Tiago et al., 2012). Moreover, we analyzed GG levels during growth of *M. hassiacum* under nitrogen limitations and also after the addition of a exogenous source of nitrogen, to confirm the trend observed in a recent study with *M. smegmatis* (Behrends et al., 2012). *Mycobacterium hassiacum* gradually accumulated GG in a nitrogen-depleted medium but upon a nitrogen upshock the GG content significantly decreased (to less that 20%). These results reinforce the existence of enzymes in mycobacterial genomes involved in the recycling of this metabolite, as source of glucose for metabolism or redirection to biosynthetic pathways, namely MGLPs assembly (Fig. 25).

We have identified the mycobacterial GG-hydrolyzing enzyme (GgH) (ZP_11162064.1) of family 63 of glycoside hydrolases and performed its biochemical characterization. While the

homologous MgHs from *T. thermophilus* and *R. raditolerans*, efficiently hydrolysed MG and GG, the recombinant GgH from *M. hassiacum* efficiently hydrolyses GG, while only trace amounts of mannose resulting from MG degradation were detected after a long period of incubation. The GgH was highly stable at 37ºC and maximally active at 42ºC. However, close to organism' optimal growth temperature (50ºC) the enzyme was less stable than the MgHs (Alarico et al., 2013). This is not unexpected considering the higher growth temperatures of the thermophies *T. thermophilus* and *R. radiotolerans*. The maximal activity of GgH was achieved at pH 5.7, a value above the optimum pH for the MgHs counterparts (4.0 and 4.5) (Alarico et al., 2013).

A few enzymes involved in GG biosynthesis show maximal activity *in vitro* at neutral pH, but are still partially active at lower pH (Costa et al., 2006; Fernandes et al., 2007). Intracellular pH required for each organism's growth is determined to some extent by extracellular pH. Although intracellular pH of *M. hassiacum* under those conditions is unknown, it may be enough for GgH activity. Furthermore, the properties of a specific enzyme *in vitro* often differ from its behaviour *in vivo* (Fernandes et al., 2010; Alarico et al., 2013). These differences may even be more pronounced between native and recombinant versions of an enzyme (Fernandes et al., 2010).

One interesting feature of GgH was the slightly high K_m values for GG, which suggests the existence of a system to control its levels only when intracellular concentration reaches the high millimolar range. This may indicate that at lower concentrations, GG may preferentially use as primer for MGLP biosynthesis, which is consistent with the much lower K_m values (below 1 mM) determined for the substrates of *M. hassiacum* GpgS, the first enzyme in the pathway (Alarico et al, unpublished). However, there are a few yeast and mycobacterial trehalases with significantly high K_m values for trehalose (34 and 20 mM, respectively). This high K_m seem to reflect accumulation of high intracellular concentrations of trehalose, which may relate to the multiple functions it may be involved, from osmotic adaptation, to protein stabilization during thermal stress or even constitutively accumulated as is the case for *Rubrobacter xylanophilus*, which accumulates very high levels possibly to uphold a high internal turgor pressure required to

counteract the elastic properties of a peptidoglycan-rich cell wall (Guyot et al., 2005; Empadinhas et al., 2007). In mycobacteria, trehalose is also part of the cell wall structure as it integrates different important glycolipids (Takayama et al., 2005; Kaur et al., 2009). Likewise, MGLP may not be the only fate for GG; it is conceivable that it may integrate other still unknown mycobacterial structures and that the activity of GgH is only "unlocked" at high GG concentrations to prevent its depletion for other essential pathways at low concentrations.

The genes for GG synthesis have been identified in all mycobacterial genomes available, but the GgH homologues were almost exclusively detected in RGM namely *M. vanbaalenii*, *M. gilvum*, *M. thermoresistibile*, *M. phlei*, *M. smegmatis*, *M. fortuitum*, *M. abscessus* and *M. massiliense*. So far, one of the few exceptions to this rule is *M. tusciae*, which is a SGM and contains a GgH homologue (Tortoli et al., 1999).

Glucose released from GG by GgH (Fig. 25) during nitrogen-limiting conditions may hypothetically support the higher growth rate of RGM over SGM under these conditions. However, nitrogen-rich macromolecules such as proteins and DNA are not likely to be efficiently synthesized without abundant nitrogen sources. Although some closely related bacteria have the machinery to fix nitrogen directly from the atmosphere, mycobacteria have not been reported to do such (Gtari et al., 2012). It is also possible that the hydrolysis of GG (the MGLP primer) by GgH may fulfil energetic requirements during nitrogen deprivation and affect a steady synthesis of MGLP. Coincidently, the RGM analysed (but not SGM) produce the related polysaccharide of methylmannose (MMP) that may functionally replace MGLP without severely compromising mycobacterial physiology in the absence of normal MGLP production (Mendes et al., 2012).

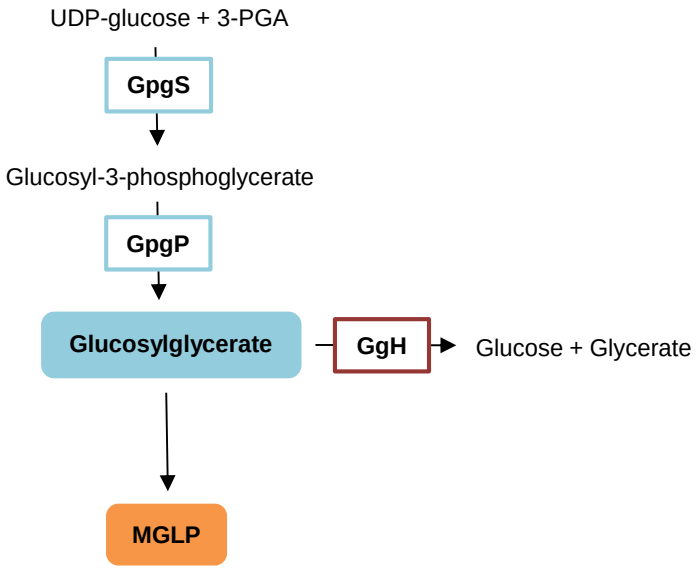

Figure 25 - Model proposed for GG hydrolysis by GgH. The blue boxes indicate enzymes involved in GG synthesis and maroon box indicate the hydrolase for GG degradation. MGLP, methylglucose lipopolysaccharide; GpgS, glucosyl-3-phosphoglycerate synthase; GpgP, glucosyl-3-phosphoglycerate phosphatase; GgH, glucosylglycerate hydrolase.

The hypothesis for a GgH-dependent decrease in GG levels upon restoration of the nitrogen levels required for *M. hassiacum* metabolism and growth has been strengthened by our results. However, there are still several interesting questions to answer namely (i) Why does GG accumulate to high levels in mycobacteria undergoing periods of nitrogen deprivation? (ii) How does nitrogen elicit GgH activation? (iii) How is the GG-hydrolyzing activity regulated during normal growth conditions? (iv) Can we expect similar results in the rare SGM carrying homologous GgH? Are there any other types of GgH in SGM, for example in *Mycobacterium tuberculosis*?

To start answering some of these questions and further our understanding of mycobacterial metabolic and physiological resources, we have elaborated an integrated research plan that will follow.

CHAPTER 5 - CONCLUSIONS

The rising numbers of human infections due to nontuberculous mycobacteria (NTM) claim for urgent measures to control these ominous pathogens. The work presented in this thesis represents an important contribution to the knowledge of mycobacterial metabolism and to the understanding of these organisms' adaptation to nitrogen-limited environments and to stress in general.

A response of *Mycobacterium hassiacum* to nitrogen-deficient conditions, an organism source of stable mycobacterial enzymes amenable to functional and structural studies, involves the accumulation of glucosylglycerate (GG), the precursor for the synthesis of MGLP, which is an important intracellular mycobacterial polysaccharide likely to regulate fatty acids synthesis.

Since efflux systems for GG have not been identified in mycobacteria, the rapid decrease in GG triggered by a nitrogen upshock is likely explained by the presence of a hydrolytic enzyme that may lead to the recycling of glucose released from GG for energetic requirements.

A new glycoside hydrolase specific for GG was identified in *M. hassiacum* and designated glucosylglycerate hydrolase (GgH). This enzyme was almost exclusively detected in rapidly-growing mycobacteria (RGM), which may relate to a high metabolic versatility of these organisms during adaptation to environmental stresses that may also be advantageous to the success of opportunistic NTM during human infection.

The biochemical properties of the GgH reported here represent a preliminary and crucial step towards future research aiming at a deeper understanding of the phenomena underlying nitrogen regulation of GG synthesis, MGLP assembly and function, and the physiological adaptation of mycobacteria to stress conditions. Intensification of research in this area will grant crucial information that may lead to the development of new and better strategies to fight the alarming numbers of diseases caused by NTM.

REFERENCES

Alarico, S., Da Costa, M. S., & Empadinhas, N. (2008). Molecular and physiological role of the trehalose-hydrolyzing α-glucosidase from *Thermus thermophilus* HB27. *J Bacteriol*, *190*(7), 2298–2305.

Alarico, S., Empadinhas, N., & Da Costa, M. S. (2013). A new bacterial hydrolase specific for the compatible solutes α-D-mannopyranosyl-(1→2)-D-glycerate and α-D-glucopyranosyl-(1→2)-D-glycerate. *Enzyme Microb Technol*, *52*(2), 77–83.

Ames, B.N. (1966). Assay of inorganic phosphate, total phosphate and phosphatases. *Methods Enzymol*, *8*, 115-118.

Banis, R. J., Peterson, D. O., & Bloch, K. (1977). *Mycobacterium smegmatis* fatty acid synthetase. *J Biol Chem*, *252*(16), 5740–5744.

Behrends, V., Williams, K. J., Jenkins, V. A., Robertson, B. D., & Bundy, J. G. (2012). Free glucosylglycerate is a novel marker of nitrogen stress in *Mycobacterium smegmatis*. *J Proteome Res*, *11*(7), 3888–3896.

Bergeron, R., Machida, Y., & Bloch, K. (1975). Complex formation between mycobacterial polysaccharides or cyclodextrins and palmitoyl coenzyme A. *J Biol Chem*, *250*(4), 1223–1230.

Cantarel, B. L., Coutinho, P. M., Rancurel, C., Bernard, T., Lombard, V., & Henrissat, B. (2009). The Carbohydrate-Active EnZymes database (CAZy): an expert resource for glycogenomics. *Nucleic Acids Res*, *37*, D233–238.

Cole, S. T., Brosch, R., Parkhill, J., Garnier, T., Churcher, C., Harris, D., Gordon, S. V., et al. (1998). Deciphering the biology of *Mycobacterium tuberculosis* from the complete genome sequence. *Nature*, *396*, 537–544.

Costa, J., Empadinhas, N., Gonçalves, L., Santos, H., Costa, M. S., & Lamosa, P. (2006). Characterization of the biosynthetic pathway of glucosylglycerate in the archaeon *Methanococcoides burtonii*. *J Bacteriol*, *188*(3), 1022–1030.

Cousins, D. V., Bastida, R., Cataldi, A., Quse, V., Redrobe, S., Dow, S., & Al., E. (2003). Tuberculosis in seals caused by a novel member of the *Mycobacterium tuberculosis* complex: *Mycobacterium pinnipedii* sp. nov. *Int J Syst Evol Microbiol*, *53*(5), 1305–1314.

De Smet, K. A. L., Weston, A., Brown, I. N., Young, D. B., & Robertson, B. D. (2000). Three pathways for trehalose biosynthesis in mycobacteria. *Microbiology*, *146*, 199–208.

Devulder, G., Pérouse de Montclos, M., & Flandrois, J. P. (2005). A multigene approach to phylogenetic analysis using the genus *Mycobacterium* as a model. *Int J Syst Evol Microbiol*, *55*, 293–302.

Dye, C. (2009). Doomsday postponed? Preventing and reversing epidemics of drug-resistant tuberculosis. *Nat Rev Microbiol*, *7*(1), 81–87.

El Helou, G., Viola, G. M., Hachem, R., Han, X. Y., & Raad, I. I. (2013). Rapidly growing mycobacterial bloodstream infections. *Lancet Infect Dis*, *13*(2), 166–174.

Elbein, A. D., Pastuszak, I., Tackett, A. J., Wilson, T., & Pan, Y. T. (2010). Last step in the conversion of trehalose to glycogen: a mycobacterial enzyme that transfers maltose from maltose 1-phosphate to glycogen. *J Biol Chem*, *285*(13), 9803–9812.

Empadinhas, N., Albuquerque, L., Henne, A., Santos, H., & Costa, M. S. (2003). The bacterium *Thermus thermophilus*, like hyperthermophilic archaea, uses a two-step pathway for the synthesis of mannosylglycerate. *Appl Environ Microbiol*, *69*(6), 3272–3279.

Empadinhas, N., Albuquerque, L., Mendes, V., Macedo-Ribeiro, S., & Da Costa, M. S. (2008). Identification of the mycobacterial glucosyl-3-phosphoglycerate synthase. *FEMS Microbiol Lett*, *280*(2), 195–202.

Empadinhas, N., & Da Costa, M. S. (2011). Diversity, biological roles and biosynthetic pathways for sugar-glycerate containing compatible solutes in bacteria and archaea. *Environ Microbiol*, *13*(8), 2056–2077.

Empadinhas, N., Mendes, V., Simões, C., Santos, M. S., Mingote, A., Lamosa, P., Santos, H., et al. (2007). Organic solutes in *Rubrobacter xylanophilus*: the first example of di-myo-inositol-phosphate in a thermophile. *Extremophiles*, *11*(5), 667–673.

Falkinham, J. O. (2009). Surrounded by mycobacteria: nontuberculous mycobacteria in the human environment. *J Appl Microbiol*, *107*(2), 356–367.

Feazel, L. M., Baumgartner, L. K., Peterson, K. L., Frank, D. N., Harris, J. K., & Pace, N. R. (2009). Opportunistic pathogens enriched in showerhead biofilms. *Proc Natl Acad Sci U S A*, *106*(38), 16393–16398.

Fernandes, C., Empadinhas, N., & Da Costa, M. S. (2007). Single-step pathway for synthesis of glucosylglycerate in *Persephonella marina*. *J Bacteriol*, *189*(11), 4014–4019.

Fernandes, C., Mendes, V., Costa, J., Empadinhas, N., Jorge, C., Lamosa, P., Santos, H., et al. (2010). Two alternative pathways for the synthesis of the rare compatible solute mannosylglucosylglycerate in *Petrotoga mobilis*. *J Bacteriol*, *192*(6), 1624–1633.

Forsberg, L. S., Dell, A., Walton, D. J., & Ballou, C. E. (1982). Revised structure for the 6-*O*-methylglucose polysaccharide of *Mycobacterium smegmatis*. *J Biol Chem*, *257*(7), 3555–63.

Fortune, S. M., & Rubin, E. J. (2007). The complex relationship between mycobacteria and macrophages: it's not all bliss. *Cell Host Microbe*, *2*(1), 5–6.

Glickman, M. S., Jacobs, W. R., York, N., & Ave, M. P. (2001). Microbial pathogenesis of *Mycobacterium tuberculosis*: Dawn of a discipline. *Cell*, *104*, 477–485.

Good, N. E., Winget, G. D., Winter, W., Connolly, T. N., Izawa, S., & Sing, R. M. M. (1966). Hydrogen ion buffers for biological research. *Biochemistry*, *5*(2), 467–477.

Gray, G. R., & Ballou, E. (1971). Isolation and characterization of a polysaccharide containing 3-*O*-methyl-D-mannose from *Mycobacterium phlei*. *J Biol Chem*, *246*(22), 6835–6842.

Gtari, M., Ghodhbane-Gtari, F., Nouioui, I., Beauchemin, N., & Tisa, L. S. (2012). Phylogenetic perspectives of nitrogen-fixing actinobacteria. *Arch Microbiol*, *194*(1), 3–11.

Guyot, S., Ferret, E., & Gervais, P. (2005). Responses of *Saccharomyces cerevisiae* to thermal stress. *Biotechnol Bioeng*, *92*(4), 403–409.

Hancock, S. M., & Columbia, B. (2007). *Glycosidases: Functions, Families and Folds*. *Encyclopedia of life sciences*. doi:10.1002/9780470015902.a0020548

Harris, L. S., & Gray, G. R. (1977). Acetylated methylmannose polysaccharide of *Streptomyces griseus*. *J Biol Chem*, *252*(8), 2470–2477.

Henrissat, B. (1991). A classification of glycosyl hydrolases based sequence similarities amino acid. *Biochem J*, *280*, 309–316.

Henrissat, B., & Bairoch, A. (1996). Updating the sequence-based classification of glycosyl hydrolases. *Biochem J*, *316*, 695–696.

Hett, E. C., & Rubin, E. J. (2008). Bacterial growth and cell division: a mycobacterial perspective. *Microbiol Mol Biol Rev*, *72*(1), 126–156.

Hunter, S. W., Gaylord, H., & Brennan, P. J. (1986). Structure and antigenicity of the phosphorylated lipopolysaccharide antigens from the leprosy and tubercle bacilli. *J Biol Chem*, *261*(26), 12345–12351.

Ilton, M., Jevans, A. W., McCarthy, E. D., Vance, D., White, H. B., & Bloch, K. (1971). Fatty acid synthetase activity in *Mycobacterium phlei*: regulation by polysaccharides. *Proc Natl Acad Sci U S A*, *68*(1), 87–91.

Jackson, M., & Brennan, P. J. (2009). Polymethylated polysaccharides from *Mycobacterium* species revisited. *J Biol Chem*, *284*(4), 1949–1953.

Jenney Jr, F. E., & Adams, M. W. W. (2008). The impact of extremophiles on structural genomics (and vice versa). *Extremophiles*, *12*, 39–50.

Jiang, S. H., Roberts, D. M., Clayton, P. a, & Jardine, M. (2012). Non-tuberculous mycobacterial PD peritonitis in Australia. *Int Urol Nephrol*.

Kalscheuer, R., Syson, K., Veeraraghavan, U., Weinrick, B., Biermann, K. E., Liu, Z., Sacchettini, J. C., et al. (2010). Self-poisoning of *Mycobacterium tuberculosis* by targeting GlgE in an α-glucan pathway. *Nat Chem Biol*, *6*, 376–384.

Kamisango, K., Dell, A., & Ballou, C. E. (1987). Biosynthesis of the mycobacterial *O*-methylglucose lipopolysaccharide. *J Biol Chem*, *262*(10), 4580–4586.

Kaur, D., Guerin, M. E., Skovierová, H., Brennan, P. J., & Jackson, M. (2009). Biogenesis of the cell wall and other glycoconjugates of *Mycobacterium tuberculosis*. *Adv Appl Microbiol*, *69*, 23–78.

Kollman, V. H., Hanners, J. L., London, R. E., Adame, E. G., & Walker, T. E. (1979). Photosynthetic preparation and characterization of ^{13}C-labeled carbohydrates in *Agmenellum quadruplicatum*. *Carbohydr Res*, *73*(1), 193–202.

Lee, J., Repasy, T., Papavinasasundaram, K., Sassetti, C., & Kornfeld, H. (2011). *Mycobacterium tuberculosis* induces an atypical cell death mode to escape from infected macrophages. *PloS One*, *6*(3), e18367.

Lee, Y. C. (1966). Isolation and characterization of lipopolysaccharides containing 6-*O*-methyl-D-glucose from *Mycobacterium* species. *J Biol Chem*, *241*(8), 1899–1909.

Lew, J. M., Kapopoulou, A., Jones, L. M., & Cole, S. T. (2011). TubercuList-10 years after. *Tuberculosis*, *91*(1), 1–7.

Lopez-Marin, L. M. (2012). Nonprotein structures from mycobacteria: emerging actors for tuberculosis control. *Clinical & developmental immunology*, *2012*. doi:10.1155/2012/917860

Maitra, S. K., & Ballou, C. E. (1977). Heterogeneity and refined structures of 3-*O*-methyl-D-mannose polysaccharides from *Mycobacterium smegmatis*. *J Biol Chem*, *252*(8), 2459–2469.

McGrath, E. E., Blades, Z., McCabe, J., Jarry, H., & Anderson, P. B. (2010). Nontuberculous mycobacteria and the lung: from suspicion to treatment. *Lung*, *188*(4), 269–282.

Mendes, V., Maranha, A., Alarico, S., Da Costa, M. S., & Empadinhas, N. (2011). *Mycobacterium tuberculosis* Rv2419c, the missing glucosyl-3-phosphoglycerate phosphatase for the second step in methylglucose lipopolysaccharide biosynthesis. *Sci Rep*, *1*(177).

Mendes, V., Maranha, A., Alarico, S., & Empadinhas, N. (2012). Biosynthesis of mycobacterial methylglucose lipopolysaccharides. *Nat Prod Rep*, *29*(8), 834–844.

Mendes, V., Maranha, A., Lamosa, P., Da Costa, M. S., & Empadinhas, N. (2010). Biochemical characterization of the maltokinase from *Mycobacterium bovis* BCG. *BMC Biochem*, *11*(21).

Murphy, H. N., Stewart, G. R., Mischenko, V. V, Apt, A. S., Harris, R., McAlister, M. S. B., Driscoll, P. C., et al. (2005). The OtsAB pathway is essential for trehalose biosynthesis in *Mycobacterium tuberculosis*. *J Biol Chem*, *280*(15), 14524–14529.

Naumoff, D. G. (2011). Hierarchical classification of glycoside hydrolases. *Biochemistry (Mosc)*, *76*(6), 622–635.

Okuyama, M. (2011). Function and structure studies of GH Family 31 and 97 α-glycosidases. *Biosci Biotechnol Biochem*, *75*(12), 2269–2277.

Pereira, P. J. B., Empadinhas, N., Albuquerque, L., Sá-Moura, B., Da Costa, M. S., & Macedo-Ribeiro, S. (2008). *Mycobacterium tuberculosis* glucosyl-3-phosphoglycerate synthase: structure of a key enzyme in methylglucose lipopolysaccharide biosynthesis. *PloS One*, *3*(11), e3748.

Phillips, M. S., & Reyn, C. F. von. (2001). Nosocomial infections due to nontuberculous mycobacteria. *Clin Infect Dis*, *33*(8), 1363–1374.

Pommier, M. T., & Michel, G. (1986). Isolation and characterization of an *O*-methylglucose-containing lipopolysaccharide produced by *Nocardia otitidis-caviarum*. *J Gen Microbiol*, *132*(9), 2433–2441.

Primm, T. P., Lucero, C. A., & Falkinham III, J. O. (2004). Health impacts of environmental mycobacteria. *Clin Microbiol Rev*, *17*(1), 98–106.

Rastogi, N., Legrand, E., & Sola, C. (2001). The mycobacteria: an introduction to nomenclature and pathogenesis. *Rev Sci Tech*, *20*(1), 21–54.

Ruffert, S., Lambert, C., Peter, H., Wendisch, V. F., & Kramer, R. (1997). Efflux of compatible solutes in *Corynebacterium glutamicum* mediated by osmoregulated channel activity. *Eur J Biochem*, *247*(2), 572–580.

Russell, D. G., Barry, C. E., & Flynn, J. L. (2010). Tuberculosis: What we don't know can, and does, hurt us. *Science*, *328*(5980), 852–856.

Sambou, T., Dinadayala, P., Stadthagen, G., Barilone, N., Bordat, Y., Constant, P., Levillain, F., et al. (2008). Capsular glucan and intracellular glycogen of *Mycobacterium tuberculosis*: biosynthesis and impact on the persistence in mice. *Mol Microbiol*, *70*(3), 762–774.

Santos, H. Lamosa, P. Borges, N., Faria, T.Q. & Neves, C. (2007). The physiological role, biosynthesis and mode of action of compatible solutes from (hyper) thermophiles. In *Physiology and Biochemistry of Extremophiles*. Gerday C. and Glandorff, N. (eds). Washington, DC, USA: ASM Press, pp. 86-103.

Sassetti, C. M., Boyd, D. H., & Rubin, E. J. (2003). Genes required for mycobacterial growth defined by high density mutagenesis. *Mol Microbiol*, *48*(1), 77–84.

Sawangwan, T., Goedl, C., & Nidetzky, B. (2009). Single-step enzymatic synthesis of (R)-2-*O*-α-D-glucopyranosyl glycerate, a compatible solute from micro-organisms that functions as a protein stabiliser. *Org Biomol Chem*, *7*(20), 4267–4270

Schröder, K. H., Naumann, L., Kroppenstedt, R. M., & Reischl, U. (1997). *Mycobacterium hassiacum* sp. nov., a new rapidly growing thermophilic mycobacterium. *Int J Syst Bacteriol*, *47*(1), 86–91.

Shinnick, T. M., & Good, R. C. (1994). Mycobacterial taxonomy. *Eur J Clin Microbiol Infect Dis*, *13*(11), 884–901.

Sinnott, M. L. (1990). Catalytic Mechanisms of Enzymic Glycosyl Transfer. *Biochem J*, *90*(7), 1171–1202.

Stadthagen, G., Sambou, T., Guerin, M., Barilone, N., Boudou, F., Korduláková, J., Charles, P., et al. (2007). Genetic basis for the biosynthesis of methylglucose lipopolysaccharides in *Mycobacterium tuberculosis*. *J Biol Chem*, *282*(37), 27270–27276.

Takayama, K., Wang, C., & Besra, G. S. (2005). Pathway to synthesis and processing of mycolic acids in *Mycobacterium tuberculosis*. *Clin Microbiol Rev*, *18*(1), 81–101.

Tamura, K., Peterson, D., Peterson, N., Stecher, G., Nei, M., & Kumar, S. (2011). MEGA5: molecular evolutionary genetics analysis using maximum likelihood, evolutionary distance, and maximum parsimony methods. *Mol Biol Evol*, *28*(10), 2731–2739.

Tiago, I., Maranha, A., Mendes, V., Alarico, S., Moynihan, P. J., Clarke, A. J., Macedo-Ribeiro, S., et al. (2012). Genome sequence of *Mycobacterium hassiacum* DSM 44199, a rare source of heat-stable mycobacterial proteins. *J Bacteriol*, *194*(24), 7010–7011.

Tortoli, E. (2009). Clinical manifestations of nontuberculous mycobacteria infections. *Clin Microbiol Infect*, *15*(10), 906–910.

Tortoli, E., Kroppenstedt, R. M., Bartoloni, A., Giuseppe, C., Pawlowski, J., & Emler, S. (1999). *Mycobacterium tusciae*. *Int J Syst Bacteriol*, *49*, 1839–1844.

Tuffal, G., Albigot, R., Rivière, M., & Puzo, G. (1998). Newly found 2-N-acetyl-2,6-dideoxy-beta-glucopyranose containing methyl glucose polysaccharides in *M. bovis* BCG: revised structure of the mycobacterial methyl glucose lipopolysaccharides. *Glycobiology*, *8*(7), 675–684.

Tuffal, G., Ponthus, C., Picard, C., Rivière, M., & Puzo, G. (1995). Structural elucidation of novel methylglucose-containing polysaccharides from *Mycobacterium xenopi*. *Eur J Biochem*, *233*(1), 377–383.

Van Ingen, J., Rahim, Z., Mulder, A., Boeree, M. J., Simeone, R., Brosch, R., & Van Soolingen, D. (2012). Characterization of *Mycobacterium orygis* as *M. tuberculosis* complex subspecies. *Emerg Infect Dis*, *18*(4), 653–655.

Weisman, L. S., & Ballou, C. E. (1984). Biosynthesis of the mycobacterial methylmannose polysaccharide: identification of a α-(1→4)-mannosyltransferase. *J Biol Chem*, *259*(6), 3457–3463.

Weiss, C. H., & Glassroth, J. (2012). Pulmonary disease caused by nontuberculous mycobacteria. *Expert Rev Respir Med*, *6*(6), 597–613.

ANNEX I

(PROTOCOLS AND SOLUTIONS)

1) GPHF medium

REAGENT	AMOUNT PER LITRE	FINAL CONCENTRATION
Glucose	10 g	55.5 mM
Tryptone	5 g	0.5%
Yeast Extract	5 g	0.5%
Beef Extract	5 g	0.5%
Calcium Chloride dehydrate	0.74 g	5 mM
Tween 80	2 g	1.52 mM

Adjust to pH 7.2 and sterilize medium by autoclaving at 120ºC, 1 atm pressure for 20 min.

2) Protocol and Solutions for DNA isolation

- Collect several colonies of *M. hassiacum* and add 400 µL of GTE buffer (see below) containing lysozyme (final concentration of 20 mg/mL). Incubate at 37ºC for 3 h at 150 rpm.

- Add 300 µL of lysis buffer (GES buffer, see below), mix and chill on ice for 10 min.

- Add 11 µL of RNAase buffer (see below), mix the tube gently and incubate in a preheated water bath at 37ºC for 60 min.

- Add 3.5 µL of Proteinase K (final concentration of 0.07 mg/mL) (Sigma-Aldrich), mix gently and incubate in a preheated water bath at 56ºC for 50 min.

- Add 250 µL of 7.5 M of ammonium acetate and chill on ice for 10 min.

- Add 100 µL of CTAB (1% CTAB/0.7 M NaCl) (Biosciences) and incubate at 65ºC for 20 min.

- Add 800 µL of chloroform/isoamyl alcohol (24:1, v/v) (AppliChem), mix manually to obtain a homogeneous mixture, centrifuge for 15 min and collect the upper phase.

- Precipitate DNA with 500 µL of 2-propanol.

- Wash two times with 500 µL 70% ethanol (centrifuge for 2 min).

- Re-suspend with 200 µL sterile water (DNAse free) and stored at 4ºC.

GTE buffer

REAGENT	AMOUNT PER 100 mL	FINAL CONCENTRATION
Glucose	0.9 g	50 mM
Tris-HCL	0.3 g	25 mM
EDTA, pH 8.0	0.4 g	10 mM

The pH was adjusted to 8.0 and the solution was sterilized through filtration and stored at 4ºC.

GES buffer

Mix 60 g of guanidine thiocyanate (AppliChem), 20 mL of EDTA 0.5 M pH 8.0 and 20 mL of sterilized ultrapure water and heat at 65ºC to complete dissolution. After cooling, add 1 g of sarcosine and water up to 100 mL. Sterilize by filtration and store at room temperature.

RNAase buffer

REAGENT	AMOUNT PER 1 mL	FINAL CONCENTRATION
RNAase A	10 mg	10 mg/mL
Tris-HCl, pH 7.5	1.2 mg	10 mM
2 M NaCl	7.5 µL	15 mM

Dissolve RNAseA in Tris-HCl buffer containing NaCl at 100ºC for 15 min to inactivate possible contamination with DNAses. Cool down the tube at room temperature before storage at -20ºC.

3) Middlebrook 7H9 medium

REAGENT	AMOUNT PER LITRE	FINAL CONCENTRATION
Di-sodium hydrogen phosphate dihydrate	2.5 g	14 mM
Monopotassium phosphate	1 g	6.4 mM
Magnesium Sulfateheptahydrate	0.5	2 mM
Calcium Chloride dihydrate	0.001 g	6.8 µM
Zinc Sulfateheptahydrate	0.001 g	3.47 µM
Ferric Citrate	0.04 g	0.163 mM
Pyridoxine	0.001 g	5.91 µM
Biotine	0.0005 g	2.046 µM
Glycerol	4 g	43.4 mM
Tween 80	1 g	0.763 mM

Heat the medium to facilitate dissolution and adjust to pH 7.2. Sterilize medium by autoclaving at 120ºC, 1 atm pressure for 20 min.

4) Agarose gel electrophoresis

- Prepare agarose gel 1% (see below).

- Load the gel with samples, containing loading buffer (Takara), and with a DNA molecular weight marker (GeneRuler™ 1kb DNA ladder, Fermentas Life Sciences).

- Run in TAE buffer 1x at 90 V for about 40 min.

Agarose Gel 1%

REAGENT	AMOUNT PER 100 mL	FINAL CONCENTRATION
Agarose	1 g	1%
TAE buffer 1x	100 mL	1x
RedSafe™ 20000x (Intron Biotechonology)	5 µL	1x

Add agarose to TAE buffer 1x (see below TAE buffer 50x) and dissolve by heating. After cooling at room temperature up to 40-50ºC add the RedSafe DNA staining solution.

TAE buffer 50x

REAGENT	AMOUNT PER LITRE	FINAL CONCENTRATION
Tris base	242 g	2 M
Acetic acid	57.1 mL	2 M
0.5 mM EDTA pH 8	100 mL	0.05 M

Dissolve Tris base in the aqueous solution of EDTA. Mix gently and heat the solution if necessary. Add the acetic acid and adjust to pH 8 with 5 M NaOH. Add distilled water at a final volume up to 1 L.

5) Competent cells

- Grow *E. coli* cells (BL21 or DH5α strains) in LB medium (see below) at 37ºC and 150 rpm, until DO_{610nm}=0.3-0.4.

- Centrifuged 10 mL of cells (in sterilized tubes) 15 min at 3000 rpm (4ºC).

- Gently re-suspend cells in 8 mL of RF1 solution (see below) and chill on ice for 15 min.

- Centrifuged 15 min at 3000 rpm (4ºC).

- Gently re-suspend cells in 2 mL of RF2 solution (see below) and chill on ice for 15 min.

- Prepare aliquots of 100 µL of cells and store at -80ºC.

RF1 Solution

Reagent	Amount per 250 mL	Final concentration
CH_3CO_2K	0.74 g	30 mM
$CaCl_2$	0.28 g	10 mM
$MnCl_2$	1.58 g	50 mM
Glycerol	37.5 mL	15%

Reagents should be added in this order and adjust to pH 5.8 with acetic acid to prevent precipitation. Sterilize by filtration.

RF2 Solution

Reagent	Amount per 50 mL	Final concentration
MOPS	0.10 g	10 mM
$CaCl_2$	0.42 g	75 mM
Glycerol	7.5 mL	15%

Adjust to pH 6.8-7 to prevent precipitation and sterilize by filtration.

6) Luria-Bertani (LB) medium

Reagent	Amount per litre	Final concentration
Tryptone	10 g	1%
Yeast Extract	5 g	0.5%
NaCl	5 g	0.5%
Agar	20 g	2.0%

Sterilize medium by autoclaving at 120ºC, 1 atm pressure for 20 min.

7) 10x Stock Salt Solution

Reagent	Amount per 100 mL	Final concentration
KCl	0.18 g	240 mM
$MgCl_2$	2 g	210 mM
$MgSO_4$	2.46 g	200 mM
Glucose	2 g	111 mM

Sterilize by filtration.

8) Buffer A (Binding Buffer)

REAGENT	AMOUNT PER LITRE	FINAL CONCENTRATION
Di-sodium hydrogen phosphate dihydrate	1.78 g	10 mM
Sodium dihydrogen phosphate dihydrate	1.56 g	10 mM
NaCl	29.22 g	0.5 M
Imidazole	1.36 g	20 mM

Adjust to pH 7.4 and sterilize by filtration.

9) Buffer B (Elution Buffer)

REAGENT	AMOUNT PER LITRE	FINAL CONCENTRATION
Di-sodium hydrogen phosphate dihydrate	1.78 g	10 mM
Sodium dihydrogen phosphate dihydrate	1.56 g	10 mM
NaCl	29.22 g	0.5 M
Imidazole	34 g	500 mM

Adjust to pH 7.4 and sterilize by filtration.

10) Protocol and Solutions for Sodium dodecylsulfate polyacrylamide gel electrophoresis (SDS-PAGE) (for additional details see Mini-PROTEAN 3 Cell Instruction Manual, BioRad, www.bio-rad.com)

- Use a glass cassette with 0.75 cm of thickness.

- Prepare the resolving gel solution (below) and let polymerize for 30 min.

- Prepare the stacking gel solution (below) insert the comb and polymerize for 30 min.

- Gently remove the comb and assemble the tank.

- Add sample buffer (dilution at least 1:2) (see below) to the samples and incubate at 95ºC for 5 min.

- Load the gel with samples and with a low molecular weight protein marker (NZYTech).

- Perform the electrophoresis with running buffer describe below at 200 V for about 40 min.

- Stain the gel with coomassie solution (see below) during 15 min at 37ºC.

- Destain gel with a proper solution (bellow) by slowly shaking the recipient.

Resolving Gel (12%)

REAGENT	AMOUNT	FINAL CONCENTRATION
Acrylamide/bis-Acrylamide, solution 29:1 (40%) (NZYTech)	1.125 mL	12%
H_2O	1.63 mL	-
1.5 M Tris-HCl pH 8.8	0.937 mL	0.4 M
Sodiumdodecylsulfate (SDS) 10% (m/v)	37.5 µL	0.1%
Ammonium persulfate (APS) 30% (w/v)	37.5 µL	0.3%
TEMED	5 µL	ND*

* Not determined

Add reagents by this order since APS and TEMED together allow gel's polymerization.

Stacking Gel (4%)

REAGENT	AMOUNT	FINAL CONCENTRATION
Acrylamide/bis-Acrylamide, solution 29:1 (40%) (NZYTech)	0.119 mL	4 %
H_2O	0.806 mL	-
0.5 M Tris-HCl pH 6.8	0.313 mL	0.1 M
Sodiumdodecylsulfate (SDS) 10% (m/v)	12.5 µL	0.1%
Ammonium Persulfate (APS) 30% (w/v)	12.5 µL	0.3%
TEMED	2.5 µL	ND*

* Not determined

Add reagents by this order since APS and TEMED together promote gel polymerization.

Sample Buffer (SDS Reducing Buffer)

REAGENT	AMOUNT PER LITRE	FINAL CONCENTRATION
H_2O	3.55 mL	-
0.5 M Tris-HCl pH 6.8	1.25 mL	0.06 M
Glycerol	2.5 mL	0.25%
SDS 10% (m/v)	2.0 mL	0.2%
Bromophenol blue 0.5% (w/v)	0.2 mL	0.02%

Store aliquots of Sample buffer at 4ºC and add 5% of β-mercaptoethanol before use.

10x Running Buffer, pH 8.3

REAGENT	AMOUNT PER LITRE	FINAL CONCENTRATION
Tris base	30.3 g	250 mM
Glycine	144 g	1.92 M
SDS	10 g	10%

Staining Solution (Coomassie Stain)

REAGENT	AMOUNT PER LITRE	FINAL CONCENTRATION
Coomassie R-250	1 g	0.1%
Glacial acetic acid	100 mL	10% (v)
Methanol	400 mL	40% (v)

Add glacial acetic acid to 500 mL of ultrapure water followed by methanol followed by the coomassie dye, stir to homogeneity and filter to remove the debris.

Destaining Solution

REAGENT	AMOUNT PER LITRE	FINAL CONCENTRATION
Methanol	250 mL	25% (v)
Glacial acetic acid	75 mL	7.5% (v)

Add glacial acetic acid to 675 mL ultrapure water followed by methanol.

11) α-naphthol/sulphuric acid reagent

REAGENT	AMOUNT
α-naphthol solution at 15% in ethanol	10.5 mL
Concentrated sulphuric acid	6.5 mL
Absolute ethanol	40.5 mL
H_2O	4.0 mL